Bioactive Materials 48 (2025) 71–99

Contents lists available at ScienceDirect

Bioactive Materials

journal homepage: www.keaipublishing.com/en/journals/bioactive-materials

Review article

Investigation into recent advanced strategies of reactive oxygen species-mediated therapy based on Prussian blue: Conceptualization and prospect

Hee-Young Kwon [a,b,1], Yuna Jung [a,1], Hojeong Jeon [a,b,**], Hyung-Seop Han [a,c,*]

[a] Biomaterials Research Center, Korea Institute of Science and Technology, Seoul, 02792, Republic of Korea
[b] KU-KIST Graduate School of Converging Science and Technology, Korea University, Seoul, 02841, Republic of Korea
[c] Research and Development Center, Elecell Corporation, Seoul, 02455, Republic of Korea

ARTICLE INFO

Keywords:
Prussian blue
Reactive oxygen species (ROS)
Antioxidant
Nanomedicine
Therapeutic agents

ABSTRACT

Prussian blue (PB) has garnered considerable scholarly interest in the field of biomedical research owing to its notably high biocompatibility, formidable multi-enzyme mimetic capabilities, and established clinical safety profile. These properties in combination with its reactive oxygen species (ROS) scavenging activity have facilitated significant progress in disease diagnosis and therapy for various ROS-mediated pathologies, where overproduced ROS exacerbates disease symptoms. Additionally, the underlying ROS-associated mechanisms are disease-specific. Hence, we systematically examined the role of ROS and its basic underlying mechanisms in representative disease categories and comprehensively reviewed the effect of PB-based materials in effectively alleviating pathological states. Furthermore, we present a thorough synthesis of disease-specific design methodologies and prospective directions for PB as a potent ROS-scavenging biotherapeutic material with emphasis on its applications in neurological, cardiovascular, inflammatory, and other pathological states. Through this review, we aim to accelerate the progress of research on disease treatment using PB-based integrated therapeutic system.

1. Introduction

Prussian Blue (PB) was created in the early 18th century by a Berlin pigment manufacturer. PB is perhaps the first synthetic pigment and one of the oldest known coordination compounds [1]. During the next three centuries, PB has transcended its traditional role as a pigment into a highly adaptable material in several advanced research fields. The PB molecular structure is $Fe_4[Fe(CN)_6]_3$ and is distinguished by a three-dimensional open framework where ferrous(II) (Fe^{2+}) and ferric (III) (Fe^{3+}) ions are systematically arranged and interconnected through cyanide ($-C\equiv N-$) ligands [2]. This specific structure helps distinguish between the insoluble and soluble PB forms, which are determined by variables such as the presence of monovalent cations (K^+, Na^+, and NH_4^+), degree of hydration (xH_2O), and potential vacancies within the $[Fe(CN)_6]^{4-}$ coordination sites. The distinctive blue color of PB is attributed to intervalence charge transfer (ICT) transitions that occurs between the Fe (II) and Fe(III) ions incorporated within its structure [3,4]. This unique three-dimensional open framework fosters rapid ion insertion and extraction, supports reversible redox reactions, and confers notable chemical stability. These factors have established PB as a highly promising material for diverse energy storage and industrial applications such as supercapacitors, displays, hydrogen storage, electrocatalysis, and sensing technologies [5–7]. Additionally, these electrochemical characteristics have expanded the application of PB to biomedical applications in recent decades, which highlights its versatility and broad potential as a multifunctional material [8–10].

In recent years, materials with diverse therapeutic objectives have been reported; these include metal-based nanosized materials (e.g., Au, Ag, and Pt NPs), metal oxide nanoparticles (e.g., Fe, Ce, Cu, and MnO_x), carbon-concluded materials (e.g., carbon nanotube; CNT, graphene oxide; GO, fullerenes), bare metal-organic frameworks (MOFs), and their derivatives [11–14]. However, PB may be one of the most promising materials among these substances because of its superior

* Corresponding author. Biomaterials Research Center, Korea Institute of Science and Technology, Seoul, 02792, Republic of Korea.
** Corresponding author. Biomaterials Research Center, Korea Institute of Science and Technology, Seoul, 02792, Republic of Korea.
E-mail addresses: jeonhj@kist.re.kr (H. Jeon), hyuhan@kist.re.kr (H.-S. Han).
[1] These authors contributed equally to this work.

https://doi.org/10.1016/j.bioactmat.2025.01.023
Received 16 January 2025; Accepted 20 January 2025

Abbreviations

ABTS	2,2′-azino-bis(3-ethylbenzothiazoline-6-sulfonic acid (ABTS)
ADP/ATP	Adenosine Diphosphate, Triphosphate
AKI	Acute Kidney Injury
AILI	Anthracycline-induced Liver Injury
AP-1	Activator Protein 1
APP	Amyloid Precursor Protein
AS	Atherosclerosis
BBB	Blood-Brain Barrier
BD	Bone-related Disease
BG	Berlin Green
BSA	Bovine Serum Albumin
CAT	Catalase
CBP	Conduction Band mediated Pathway
CD	Cluster of Differentiation
CDK5	Cyclin-Dependent Kinase 5
CS	Chitosan
CVD	Cardiovascular Diseases
Cyt C	Cytochrome C
DAMP	Damage-Associated Molecular Pattern
DJ-1	Protein Deglycase DJ-1
DFU	Diabetic Foot Ulcers
ER	Endoplasmic Reticulum
FDA	Food and Drug Administration
GSK-3	Glycogen Synthase Kinase 3
HMGB-1	High Mobility Group Box-1
IBD	Inflammatory Bowel Disease
ICAM-1	Intercellular Adhesion Molecule 1
ID	Inflammatory Diseases
IFN-γ	Interferon-gamma
IL	Interleukin
iNOS	inducible Nitric Oxide Synthase
IRI	Ischemia-Reperfusion Injury
IAEA	International Atomic Energy Agency
IVD	Intervertebral Disc
JNK-AP1	Jun N-terminal Kinase-Activator Protein 1
KEAP1	Kelch-like ECH-Associated Protein 1
KGM	Konjac Glucomannan
LFA-1	Lymphocyte Function-associated Antigen 1
LRRK-2	Leucine-Rich Repeat Kinase 2
M1	Type 1 Microglia
M2	Alternative Activated Macrophage
Mac-1	Macrophage-1 antigen
MAF	Musculoaponeurotic Fibrosarcoma
MAPKs	Mitogen-Activated Protein Kinases
MMPs	Matrix Metalloproteinases
mPTP	mitochondrial Permeability Transition Pore
MSCs	Mesenchymal Stem Cells
ND	Neurological Diseases
NF-κB	Nuclear Factor kappa-light-chain-enhancer of activated B cells
NET	Neutrophil Extracellular Traps
NIR	Near-Infrared
NOX2	NADPH Oxidase 2
Nrf2	Nuclear Factor Erythroid 2-Related Factor 2
OF	Organ Failure
OS	Osteoarthritis
Oxi-LDL	Oxidized Low-Density Lipoprotein
PAF	Platelet Activating Factor
PB	Prussian Blue
PBA	Prussian Blue Analogs
PDT	Photodynamic Therapy
PEG	Polyethylene Glycol
PEI	Polyethyleneimine
POD	Peroxidase
PP	Protein Phosphatase
PINK1	PTEN-Induced Putative Kinase 1
P-sel	P-selectin
PTT	Photothermal Therapy
PVP	Polyvinylpyrrolidone
PVA	Polyvinyl Alcohol
PW	Prussian White
PY	Prussian Yellow
RBCs	Red Blood Cells
ROS	Reactive Oxygen Species
SCI	Spinal Cord Injury
SMCs	Smooth Muscle Cells
SOD	Superoxide Dismutase
TB	Thrombosis
TNF-α	Tumor Necrosis Factor-alpha
TMB	3,3′,5,5′-Tetramethylbenzidine
TOM20	Translocase of Outer Membrane 20
TXA2	Thromboxane A2
VBP	Valence Band mediated Pathway
VCAM-1	Vascular Cell Adhesion Molecule 1
VSMC	Vascular Smooth Muscle Cells
vWF	von Willebrand Factor
WH	Wound Healing

biocompatibility and therapeutic efficacy [15]. The significant merit of PB that makes it suitable for biomedical applications is its clinically established safety profile, which has been highlighted by the endorsement of the U.S. Food and Drug Administration (FDA) as an antidote for heavy metal poisoning and its inclusion in the World Health Organization (WHO) essential medicines catalog [16]. In addition to its clinical safety, PB exhibits numerous attributes such as high biocompatibility, minimal toxicity, substantial surface area, catalytic efficacy, and distinctive photothermal and magnetic properties. These attributes have acted as significant factors in facilitating the innovation of an advantageous versatile nanoplatform that is applicable in various areas including bioimaging, biosensing, oncological treatment, and targeted pharmaceutical delivery. As a biotherapeutic agent, PB exhibits notable biological effectiveness as a nanozyme; hence, it proficiently scavenges the reactive oxygen species (ROS) that are produced in excess under pathological conditions associated with diverse diseases. ROS act as pivotal intermediates in a broad spectrum of physiological and pathological processes. Furthermore, their effects and underlying mechanisms differ considerably across various diseases; hence, they are often used as vital biomarkers for diagnostic purposes and therapeutic interventions [17,18]. Furthermore, unlike other biomaterials that generally function as mono- or dual-nanozymes, PB functions as a multifunctional nanozyme that mimics the enzymatic activities of natural antioxidants such as superoxide dismutase (SOD), peroxidase (POD), and catalase (CAT) [19]. This multi-enzymatic functionality enables PB to play an active role in the detection and regulation of ROS-associated pathways. Additionally, this enhances its extensive applicability in the management of a wide array of conditions that encompass neurological, cardiovascular, and inflammatory disorders. However, despite its considerable therapeutic promise, the advancement of novel PB-based materials in therapeutic applications has been hindered by distinct challenges. Therefore, gaining an accurate comprehension of the underlying disease-specific mechanisms that govern ROS production and formulating appropriate synthetic

methodologies are imperative for establishing PB as a leading ROS-scavenging therapeutic agent. This strategic approach is required to create customized translational nanomedicines that are compatible with the unique pathological characteristics that are inherent to each disease (Fig. 1).

2. Oxidative stress in diseases

Decades of comprehensive investigation has conclusively established that oxidative stress is a crucial determinant in a myriad of diseases and contributes to decreased mortality rates [20,21]. Both exogenous and endogenous factors induce the excessive generation of reactive gaseous molecules (reactive oxygen/nitrogen species; ROS or RNS), which cause irreversible biomolecular alteration and cellular or tissue structural damage [22–25]. Briefly, an imbalance in ROS and RNS levels triggers oxidative stress, which predominantly leads to further generation of ROS or RNS molecules such as hydroxyl radicals (•OH), superoxide anions ($\bullet O^{2-}$), hydrogen peroxide (H_2O_2), nitric oxide (•NO), nitrogen dioxide radicals ($\bullet NO_2$), nitrate radicals ($\bullet NO_3$), and peroxynitrite ($ONOO^-$) [26,27]. Superoxide anions may further react with H_2O_2 and •NO and produce highly reactive •OH and $ONOO^-$ [28]. These reactive species incite substantial oxidative damage within biological systems [29]. The abundance of these species correlates with disease pathogenesis and progression in neurological, cardiovascular, and inflammatory diseases and cancer [30–32]. From a clinical perspective, oxidative stress has been predominantly managed by administering antioxidants to mitigate the effects of oxidative processes within the organism [33–35]. Nevertheless, the indiscriminate use of antioxidants has been recently suggested to inadvertently result in cellular damage or disruption of pivotal signaling pathways within biomolecules [36–38]. This emergent understanding accentuates the necessity of preserving a delicate equilibrium between oxidants and reductants to sustain overall health [39–41]. This paradigm shift has spurred several studies to comprehend and avert oxidative imbalances [41].

An understanding of oxidative homeostasis has significantly shown that specific ROS and RNS are crucial mediators of intracellular signaling and physiological processes that play vital roles in sustaining life [42]. Based on this insight, a new classification of oxidative stress has been implemented to distinguish between "oxidative eustress" and "oxidative distress" [43–45]. Oxidative eustress refers to the physiological role of redox signaling, where endogenous oxidants function at appropriate levels and contribute to cellular homeostasis and signaling through normal metabolic activities (Fig. 2) [45]. In contrast, oxidative distress occurs when endogenous or exogenous oxidants are overproduced at a rate that surpasses the capacity of the antioxidant defense mechanisms in the body [46]. This imbalance results in significant damage to nucleic acids (NA), proteins, and lipids and may lead to mitochondrial dysfunction, dysregulation of cellular signaling pathway, and high risk of tumor formation. Hence, understanding and managing the delicate balance between oxidative eustress and distress is critical for developing targeted therapeutic strategies [47].

This review presents a comprehensive analysis of the findings of contemporary studies on mitigating ROS overproduction in various pathological contexts. It primarily expounds the heterogeneous PB synthesis methodologies that have been specifically engineered to target distinct diseases. Furthermore, the underlying mechanisms of ROS modulation have been explained with respect to different diseases. This review advocates systematic approaches in the design of PB for the

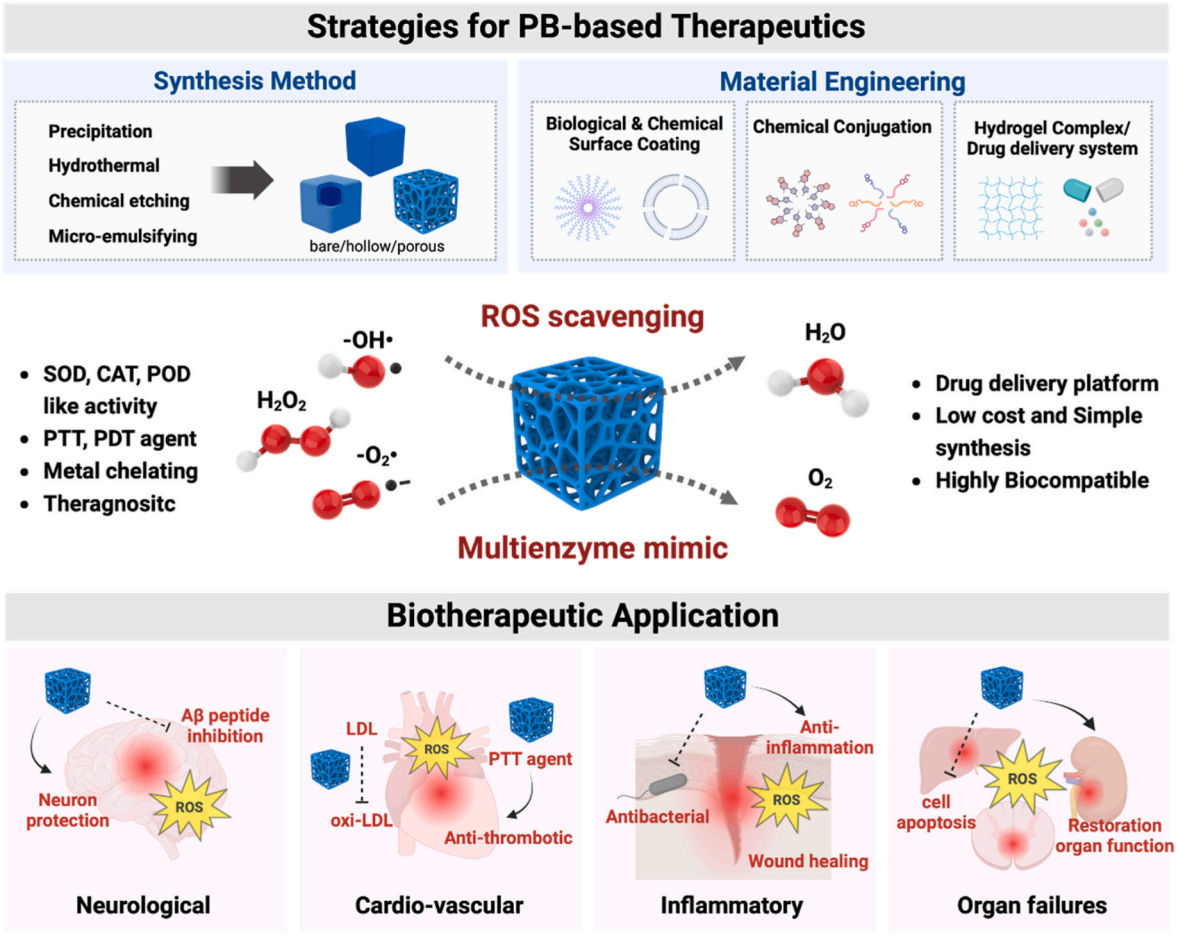

Fig. 1. Schematic of Prussian Blue-based biotherapeutics and their applications.

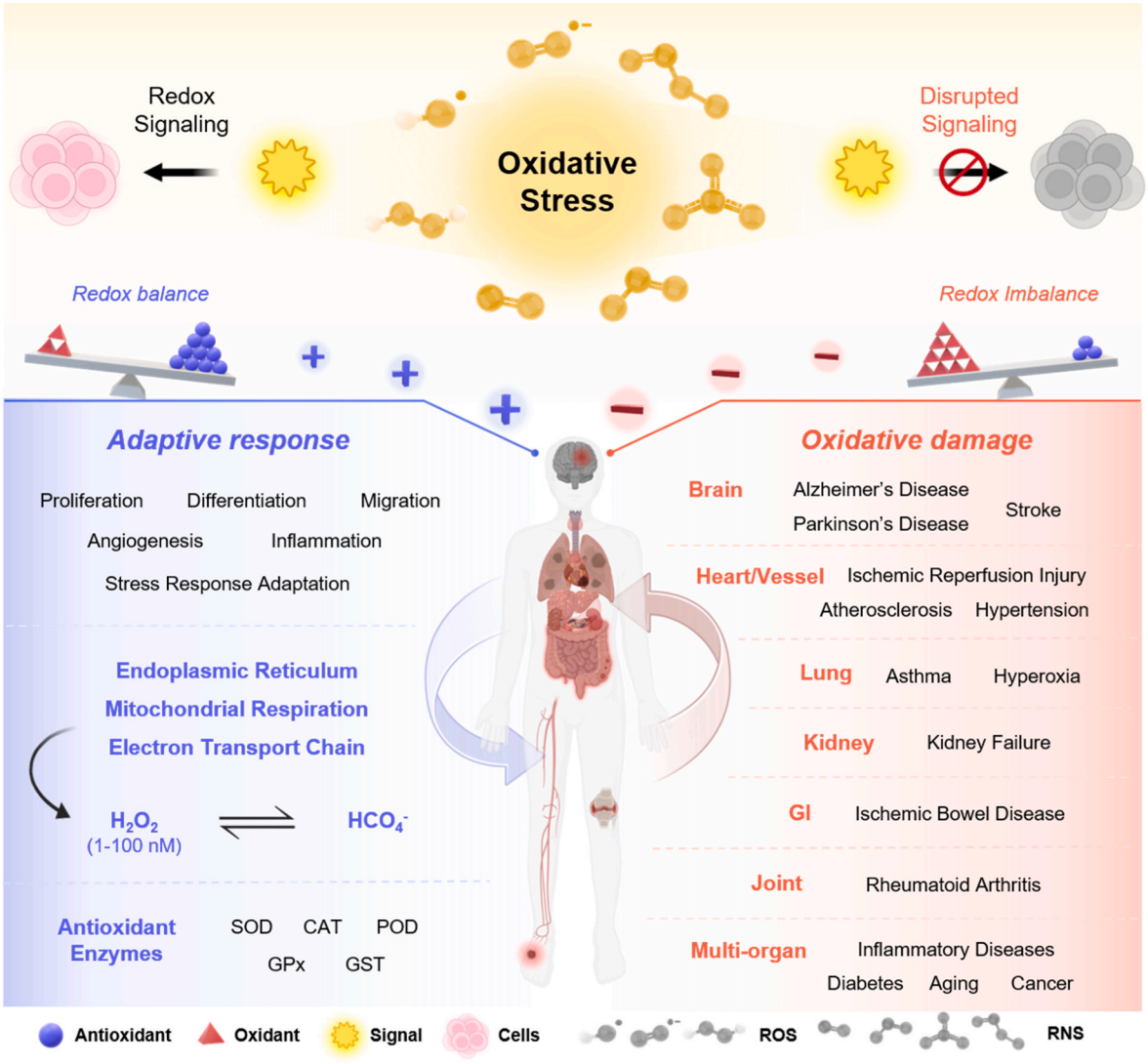

Fig. 2. Fundamentals of oxidative stress homeostasis in human body and its association with various diseases.

effective preservation of oxidative stress homeostasis. This perspective aims to establish a foundational framework for future queries regarding the formulation of PB-based biotherapeutic agents for ROS scavenging across a spectrum of diseases and simultaneously provide essential insights to researchers for the advancement of this field of study.

3. PB-associated catalytic mechanism

PB exhibits a range of redox states such as Prussian Blue (PB), Prussian White (PW), Berlin Green (BG), and Prussian Yellow (PY). Each state is distinguished by unique redox potentials [19]. This variation in redox state can be attributed to the diverse oxidation states of iron, which are modulated both by high-spin Fe^{2+}/Fe^{3+} and low-spin $Fe(CN)_6^{3-}/Fe(CN)_6^{4-}$ configurations [48]. The fluctuation in redox potential profoundly influences the crystalline architecture of PB, which facilitates its role as an efficient electron transfer mediator. This augments its capacity to scavenge ROS [49,50]. PB elicits superoxide dismutase (SOD)-like activity by eliminating superoxide, accepting electrons from it, and converting it into molecular oxygen (**Reaction 1**) [19]. Subsequently, the reduced PB form undergoes oxidation by another superoxide molecule or reactive species present in the system, eventually resulting in the reduction of superoxide to hydrogen peroxide (**Reaction 2**). This underlying mechanism effectively alleviates the effects of superoxide by transforming it into less reactive species, specifically oxygen and hydrogen peroxide (**Reaction 3**). During this process, PB closely emulates the functionality of SOD enzymes by catalyzing the disproportionation of superoxide. Thus, its ability to oscillate between its oxidized and reduced forms enables it to maintain the catalytic cycle, which is supported by its extensive redox potentials.

$$PB + O_2^- \rightarrow PB\ (red) + O_2 \quad (1)$$

$$PB\ (red) + O_2^- + 2H^+ \rightarrow PB + H_2O_2 \quad (2)$$

$$2O_2^- + 2H^+ \rightarrow O_2 + H_2O_2 \quad (3)$$

Furthermore, the hydrogen peroxide that is produced as a secondary product of the SOD-like mechanism is proficiently removed through the sequential actions of POD-like and CAT-like functionalities of PB [51]. The POD-like mechanism involves PB-mediated electron transfer, which reduces hydrogen peroxide by oxidizing various electron donor substrates such as 2,2′-azino-bis(3-ethylbenzothiazoline-6-sulfonic acid (ABTS) and 3,3′,5,5′-Tetramethylbenzidine (TMB) [52]. In this mechanism, PB is reduced by accepting electrons from these substrates. Subsequently, the reduced PB reacts with hydrogen peroxide, which facilitates electron transfer. Thus, PB reverts to its oxidized form, whereas hydrogen peroxide simultaneously undergoes reduction and is decomposed into water (**Reaction 4**) [53]. In the context of CAT-like

functionality, PB catalyzes the direct decomposition of hydrogen peroxide, which yields water and oxygen [19]. Thus, PB is oxidized by hydrogen peroxide, whereas hydrogen peroxide is concurrently reduced to water, following which the oxidized PB is reduced by its interaction with an additional hydrogen peroxide molecule that is oxidized to oxygen (**Reaction 5**). Notably, distinct electron transfer pathways exist in both the POD and CAT-like mechanisms; however, PB uniformly functions as an electron transfer mediator in both processes. It undergoes cyclic oxidation–reduction processes, which is a critical catalytic function in the decomposition of hydrogen peroxide.

$$PB + substrate \rightarrow PB\ (oxi) + substrate^{\bullet+} + H_2O_2 \rightarrow PB + substrate^{\bullet+} + H_2O \quad (4)$$

$$PB + H_2O_2 \rightarrow PB\ (oxi) + H_2O + H_2O_2 \rightarrow PB + H_2O + O_2 \quad (5)$$

The mechanisms underlying POD and CAT-like activities of PB have been clarified recently. They involve two distinct electron transfer pathways: the valence band-mediated pathway (VBP) and conduction band-mediated pathway (CBP) (Fig. 3) [54]. The VBP involves the oxidation of PB by transferring electrons to H_2O_2, followed by its reduction by the acceptance of electrons from ABTS to complete the cycle. In contrast, the CBP involves the reduction of PB by receiving electrons from ABTS while subsequently undergoing oxidation by donating electrons to H_2O_2. As both are recurring processes, PB is recycled between these states. Both VBP and CBP are essential for POD-like activity, whereas CBP is primarily responsible for CAT-like activity. Notably, both pathways may operate concurrently, and the dominant pathway is determined by the PB oxidation state and specific reaction conditions. Furthermore, irreversible pre-oxidation by H_2O_2 significantly enhances both POD and CAT activities. This enhancement is attributed to the increase in the oxidation state of ferric ion (Fe^{3+}) and generation of oxygen-containing functional groups (−OH, =O) on PB surface, which extends the cycle life.

4. PB synthesis strategies for various diseases

PB can be prepared using numerous synthesis methods such as precipitation, co-precipitation, hydrothermal synthesis, microemulsion techniques, and other advanced approaches [55–58]. Several extensive studies have been conducted in the energy field to enhance synthesis yield, regulate particle size and structural morphology, and improve the intrinsic efficiency of PB particles [59–61]. Additionally, PB is now considered a promising substitute for biocatalysts, and efforts have been increasingly focused on developing multifunctional strategies to enhance its catalytic activity and biocompatibility for biomedical applications [62]. Therefore, conventional synthesis methods have been modified to optimize the *in vivo* catalytic performance and biological compatibility of PB.

This section presents a comprehensive overview of PB synthesis techniques and summarizes the surface modification and functionalization strategies designed to enhance its biocompatibility and ROS scavenging efficiency (Fig. 4, Fig. 5, Table 1).

4.1. Precipitation and modified precipitation

PB may be effectively synthesized using precipitation methods, which are among the most straightforward techniques available [63]. These methods are classified as direct precipitation and co-precipitation based on the number of iron ion sources used (Fig. 4a).

During direct precipitation, iron ion is obtained from a single source [64], and PB is synthesized from the reaction between the representative transition metal salts (e.g., $FeCl_2$, $FeCl_3$) and hexacyanoferrate ion ($[Fe(CN)_6]^{4-}$) in a solvent [65]. In contrast, two or more sources of iron ions are used during co-precipitation [57]. However, both approaches are categorized as precipitation methods. Direct precipitation typically involves the reaction of transition metal salts with $[Fe(CN)_6]^{4-}$ in solution to produce PB. In contrast, co-precipitation incorporates additional iron sources, such as hexacyanoferrate (II/III) salts (e.g., $[Fe(CN)_6]^{4-}$, $[Fe(CN)_6]^{3-}$) and iron(II/III) salts (e.g., $FeCl_2$, $FeCl_3$). The reaction leading to the formation of a precipitate or colloidal suspension is normally influenced by the molar ratios of these salts. The first step in this process involves the formation of PW ($Na_2Fe[Fe(CN)_6]$), which precipitates as an intermediate. This intermediate product subsequently undergoes oxidation *via* a second step and is converted into PB [66].

However, although co-precipitation stabilizes reactant concentrations, it often induces structural defects in the synthesized PB because of the rapid precipitation rate [67]. To address this issues, novel synthetic methods and combinations have been suggested to enhance PB quality and functionality. Another intrinsic challenge associated with PB synthesis is its tendency to aggregate in aqueous solutions, resulting in instability [68]. Furthermore, immune responses are triggered when aggregated PB is introduced into biological systems. Hence, this is a critical factor that needs to be addressed [69]. Surface-functionalized synthesis methods are now widely adopted to enhance PB bioactivity. Polymers (e.g., natural biopolymers, synthetic chemical polymers), organic acids, and intrinsic biomolecules have been used to solve those problems with polyvinylpyrrolidone (PVP), polyvinyl alcohol (PVA), polyethyleneimine (PEI), and polyethylene glycol (PEG) being the most commonly applied polymers [63,70,71]. To produce uniform-sized PB nanoparticles (PBNPs), the selected polymer is stirred with ferrous or ferric ion-containing solutions in situ, followed by the addition of hexacyanoferrate. Moreover, the physical properties of PB are optimized by adjusting the polymer-to-iron ion ratio or reaction temperature [72]. These modifications have been proven to be distinctly beneficial for the use of PB in biomedical applications where material stability, biosafety, and functional versatility are of paramount importance [73,74].

Bare PB is synthesized through direct precipitation. It has been extensively studied for its potential applications in addressing a broad spectrum of human diseases including neurological diseases,

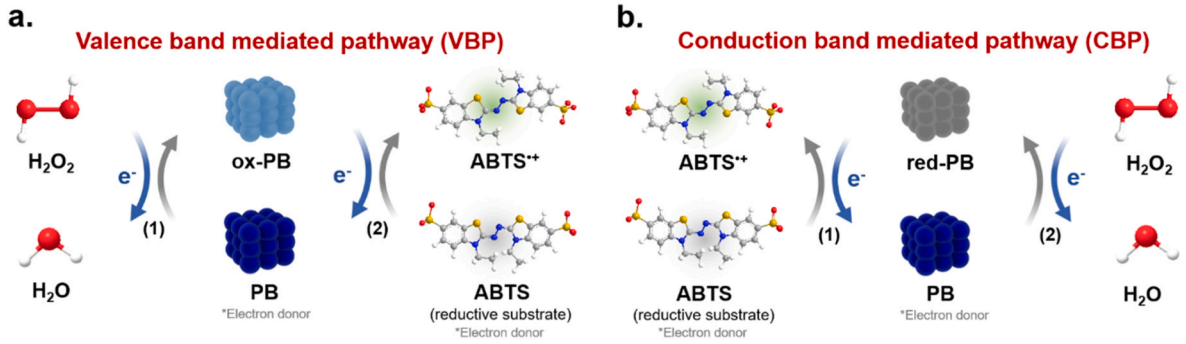

Fig. 3. PB dual electron transfer pathway with H_2O_2 catalysis. (a) Valence band-mediated pathway (VBP). (b) conduction band-mediated pathway (CBP). Reprinted with permission [54] copyright 2024. Springer Nature.

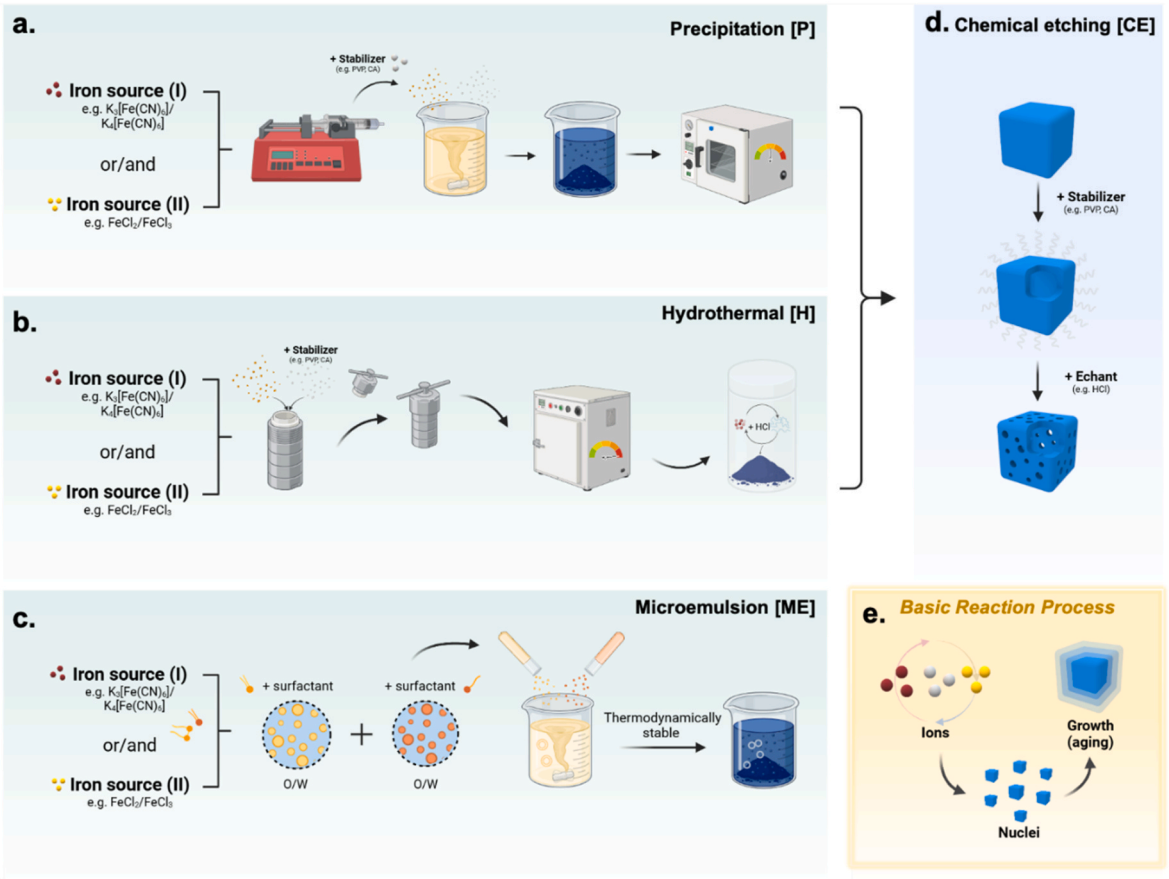

Fig. 4. Representative methods of Prussian Blue synthesis for ROS-related diseases therapy. (a) Precipitation method [P], (b) Hydrothermal method [H], (c) Microemulsion method [M], and (d) Chemical etching [CE]; (e) basic reaction process of PB synthesis.

cardiovascular diseases, inflammation, and organ failures (e.g., kidney, lung, liver) [75–78]. Bare PB is synthesized using potassium ferricyanide ($K_3[Fe(CN)_6]$) as the iron ion donor, hydrochloric acid (HCl) to create an acidic environment, and poly(vinylpyrrolidone) (PVP) as the reducing agent to intensify physiological stability. Between 2022 and 2023, Liu et al. and Ma et al. successfully synthesized crystalline PB that was approximately 100–110 nm in size using this method [79,80]. The synthesized PB showed antioxidant, anti-inflammatory, and anti-apoptotic properties; elicited neuroprotective effects in stroke mouse models, and alleviated Parkinson's disease (PD) progression by inhibiting pyroptosis. Furthermore, PB was synthesized at varied sizes and morphologies by altering the reaction parameters such as time, temperature, and solvent condition. These PB particles have been used to alleviate atherosclerosis (AS), ischemia-reperfusion injury (IRI), inflammatory bowel disease (IBD), and organ failure (OF). Notably, Qin et al. produced ultrasmall PB particles by altering the solvent composition to 75 % ethanol to induce structural rearrangement in the PVP molecular chains [81]. This innovative approach was proposed as a novel strategy for osteoarthritis (OS) treatment.

Lately, advanced strategies have been used to functionalize PB that has been synthesized *via* direct precipitation to improve its biological affinity and cellular uptake and achieve drug delivery and targeted therapy. Recent advances in PB-based ROS scavenging strategies fall roughly into three approaches.

The first approach involves coating bare PB with cell membranes. In 2021, Feng et al. obtained differentiated HL-60 cells derived from the peripheral blood progenitor cells of patients with acute leukemia to coat the surface of PBNPs with cell membranes [82]. This biomimetic technique preserved the intrinsic properties of the particle core while imparting additional biological activity. Modification of the particle surface with specific cell membranes significantly improved their accumulation at target sites and acted as an efficient platform for targeted delivery. The second approach involves coating with biopolymers. In 2024, Zhao et al. used this approach to coat PB with polydopamine [83]. This *in vivo* study was conducted in an ischemic stroke animal model, and it has highlighted the therapeutic potential of this approach. They manufactured newly engineered PBNPs using a one-step precipitation method and dispersed them in Tris-HCl buffer (10 mM, pH 8.5). Then, dopamine hydrochloride was polymerized onto PB surface using the relatively conventional ultrasonication technique. This biopolymer-coated PB effectively targeted neuronal mitochondria and significantly alleviated ischemic stroke symptoms.

Thirdly, during atherosclerosis (AS) therapy, Zhou et al. directly precipitated PB by pay-loading with the chemical drugs Artemisinin (ART) and Procyanidins (PC) [84]. They fabricated porous PBNPs known as hollow PB using chemical etching. Then, they coated the hollow PB with macrophage and red blood cell membranes. This multifaceted surface engineering approach effectively delivered PB to atherosclerotic plaques and ensured targeted drug release while facilitating complete drug clearance from the bloodstream. A similar strategy was used by Liu et al., who pay-loaded multiple drugs onto PBs and functionalized the surfaces with the synthetic polysaccharide dextran [85,86]. This modification improved the drug-delivery efficiency to ischemia-reperfusion injury (IRI) sites and promoted the polarization of macrophages into the M2 phenotype. These examples highlight the fact that the precipitation method while simple is cost-effective, reliable, and particularly amenable to various surface modification strategies [86]. Thus, it has yielded a more significant body of study outcomes compared with those of other synthetic methods.

Recent studies on co-precipitation methods to develop Prussian Blue

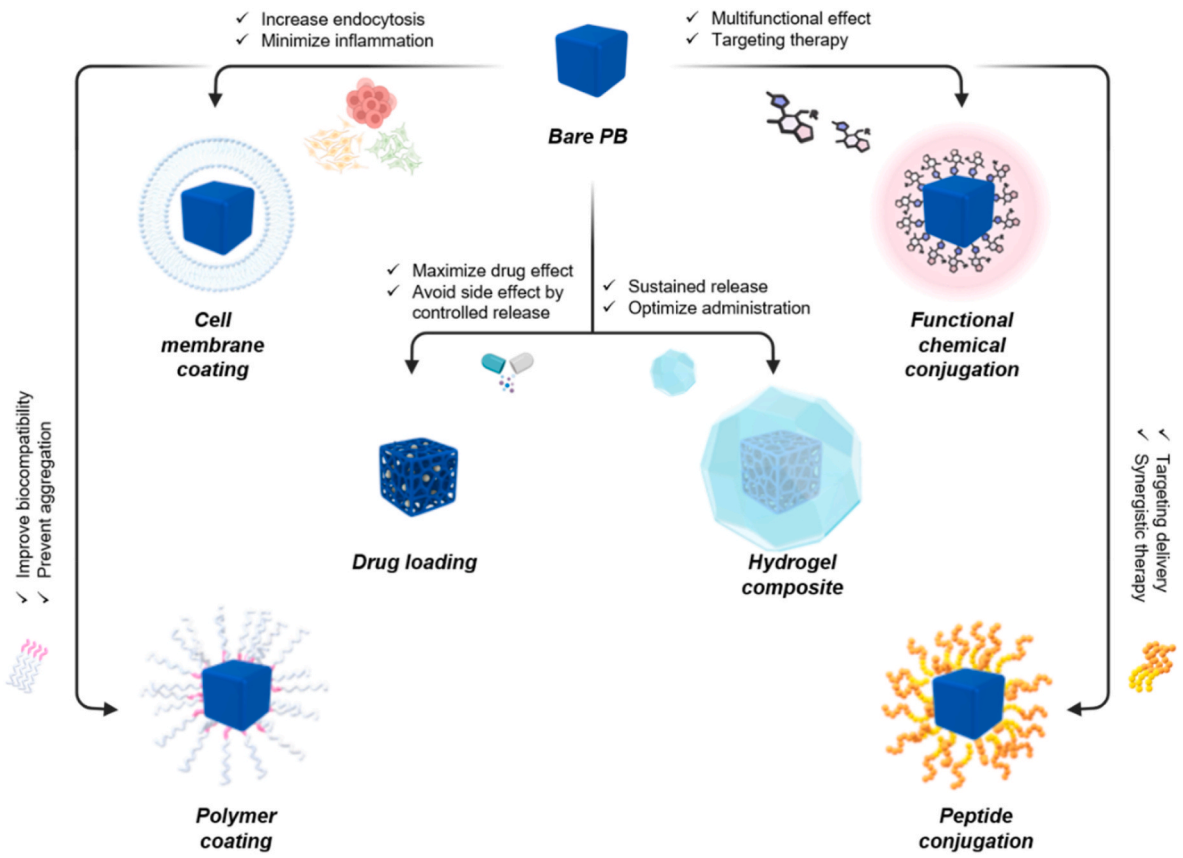

Fig. 5. Illustration of combinational strategies using Prussian Blue to amplify ROS-scavenging and therapeutic effect.

analogs (PBAs) have also gained attention. However, this review primarily focuses on specific PB forms that are considered most biocompatible for biological applications—such as those with cores containing K^+ and Na^+. The co-precipitation technique is defined here as "modified precipitation," and it offers precise control over the growth of the PB crystal, which enables relatively rapid reactions. Therefore, this approach is highly suitable for large-scale production [87]. Kowalczyk et al. synthesized PBNPs that were approximately 110 nm in size using citric acid as the stabilizer instead of PVP and selecting $FeCl_3$ and $K_4[Fe(CN)_6]$ as co-providers of iron ions [88]. Under similar conditions, Zhao et al. produced a PB complex that was enhanced with manganese ions (Mn) and showing improved efficiency in scavenging ROS [89].

Additionally, the modified precipitation method may be combined with various surface engineering techniques. Li et al. successfully encapsulated PBs using red blood cell membranes to extend the circulation time in the bloodstream and intensify its ability for specific accumulation at pathological sites [90]. Furthermore, they subjected near-infrared (NIR) irradiation to temporarily enlarge the blood–brain barrier (BBB) penetration probability of PBs and lower the aggregation of amyloid-beta fibrils. Tong et al. developed a biomimetic PB system by growing PB in bovine serum albumin (BSA) nanobubbles and loading therapeutic agents into the materials [91]. Additionally, they introduced a chemical modification step to conjugate the photosensitizer chlorin6 (Ce6) by carboxylating (–COOH) the PBs. The functionalized PB was used in a photodynamic therapy (PDT) strategy for treating diabetic foot infections. Zhang et al. used PB for thrombolysis intervention by developing a synthesis strategy for loading at the core of hollow PB with perfluorinated pentane (PFP) as the photothermal therapy (PTT) reagent and conjugating it with fibrin-binding peptides on the surface [92,93].

In 2023, Shen et al. adapted this approach for treating spinal cord injury (SCI). This demonstrates the potential of this therapeutic approach for application under different pathological contexts [94]. Zhang et al. suggested the use of an in situ biopolymer coating method using chitosan (CS) to develop a cure for acute kidney injury (AKI) [95]. This approach enhanced the biocompatibility and physiological stability of PB, making it suitable for AKI treatment.

In summary, disease-specific PB designs based on precipitation methods may appear simple and straightforward. However, they also act as a foundation for creating versatile combinations of PB, which enables innovative approaches to therapeutic applications.

4.2. Hydrothermal method

After precipitation, hydrothermal synthesis is among the most frequently used synthesis methods. It is distinguished by its requirement for a sealed high-temperature high-pressure environment (Fig. 4b) [96,97]. The stringent reaction parameters significantly promote hydrolysis, oxidation, and crystallization of the reactants, thereby notably improving both the reactivity and overall efficacy of the procedure. In this approach, $[Fe(CN)_6]^{4-}$, which is used as the single iron source material, undergoes dissociation under acidic and high-temperature conditions to yield Fe^{3+} and Fe^{2+} ions. Subsequently, the released iron ions react with residual $[Fe(CN)_6]^{4-}$ to produce PB.

Owing to the slow rate of Fe^{2+} release, PB yield is generally lower compared with those of co-precipitation methods [98]. Moreover, the characteristic of this method to enable gradual crystallization leads to diminished crystallinity and augmented porosity, which consequently improves the stability and specific capacity of the substance [99].

However, in spite of its comparative ease of implementation, this strategy presents inherent risks because of the volatilization of hydrogen cyanide (HCN), which is an exceedingly toxic substance [100]. Hence, modified hydrothermal synthetic methods that incorporate additives such as PVP, ascorbic acid, or NaCl have been developed to overcome these challenges [101,102]. Thus, these modifications improve process

Table 1
Prussian Blue synthesis and modification strategies according to the disease.

Synthesis strategy	Prussian Blue form	Synthesis condition (Reaction time, Temperature/Pressure)	Surface engineering condition	Engineering advantages	Size	Ref
Precipitation [P]	PBzyme	(i) PVP, $K_3[Fe(CN)_6]$, HCl, Stirring, RT, 2 h (ii) 80 °C oven incubation, 24 h	**[Bare Surface]**	n.r.	~100 nm (square)	[79]
	PBzyme	(i) PVP, $K_3[Fe(CN)_6]$, HCl, Stirring, RT (ii) 80 °C oven incubation, 20 h		n.r.	~106 nm (circle)	[80]
	n-PBEs	(i) PVP, $K_3[Fe(CN)_6]$, HCl, stirring, RT, 1 h (ii) 80 °C oven incubation, 24 h		n.r.	~100 nm (mix of square and circle)	[75]
	PBzyme	(i) PVP, $K_3[Fe(CN)_6]$, HCl, stirring, RT, 1 h (ii) 80 °C oven incubation, 24 h		n.r.	~65 nm (circle)	[76]
	PB Scavengers	(i) PVP, $K_3[Fe(CN)_6]$, HCl, stirring, RT (ii) 80 °C oven incubation, 20 h		n.r.	~80 nm (circle)	[115]
	USPBNPs	(i) PVP, $K_3[Fe(CN)_6]$, HCl, 75 % EtOH, Stirring (ii) 80 °C oven incubation, 3 h (iii) Ultrafiltration		n.r.	~3.5 nm	[81]
	PBNPs	(i) PVP, $K_3[Fe(CN)_6]$, HCl, stirring, RT (ii) 100 °C, 20 h		n.r.	~160 nm (square)	[77]
	PBZs	(i) PVP, $K_3[Fe(CN)_6]$, HCl, stirring, 30 min (ii) 80 °C incubation, 20 h		n.r.	~119 nm (square)	[78]
Precipitation/Post-modification [P]+[M]	MPBzyme@NCM	(i) PVP, $K_3[Fe(CN)_6]$, HCl, Stirring, RT, 2 h (ii) 80 °C oven incubation, 24 h	**[Cell membrane coating]** (i) Differentiated HL-60 cells, salin, extruder (100 nm PC filtered)	- Neutrophil-like targeting effect - Improving PB delivery	~160 nm (mix of square and circle)	[82]
	PB@PDA	(i) PVP, $K_3[Fe(CN)_6]$, HCl, stirring, RT, 30 min (ii) 80 °C oven incubation, 20 h	**[Polydopamine coating]** (i) Dopamine-HCl, pH 8.5 Tris-HCl, stirring, 25 °C, 1 h	- Promoting cell adhesion, proliferation, differentiation of nerve cells	~115 nm (square)	[83]
	HA-M@PB@ (PC + ART)	(i) PVP, $K_3[Fe(CN)_6]$, HCl, stirring, 80 °C, 20 h	**[Cell membrane coating/Drug loading]** (i) RAW264.7, RBC membrane, sonication, 5 min, stirring, 37 °C, 1 h (ii) PB@PC or ART, 70 % EtOH, stirring, RT, 24 h (iii) PB@PC:PB@ART (1:10 ratio), membrane (1:1, RAW264.7: RBC), extruder (iii) Add HA-PEG2000-DSPE into previous NPs	- Localizing NPs to atherosclerotic plaques - Prolonging circulation time and improving drug accumulation in diseased regions	~150 nm (mix of square and circle)	[86]
	DSS/PB @BSP	(i) PVP, $K_3[Fe(CN)_6]$, HCl, stirring, RT, 30 min (ii) 80 °C oven incubation, 24 h	**[Multi-drug loading]** (i) PB, BSP solution (or Cy5), shaking, 24 h (ii) PB@BSP, DSS, stirring, 30 min	- Targeting ligand for scavenger receptor on MN - Reprograming them into M2 macrophages for enhanced therapy of MI/RI - Anti-inflammation	~100 nm (crystal)	[85]
Precipitation /Chemical etching /Post-modification [P]+[E]+[M]	HMPB-rtPA@PM	(i) PVP, $K_3[Fe(CN)_6]$, HCl, stirring, RT, 30 min (ii) 80 °C oven incubation, 24 h (iii) PB, PVP, HCl, Stirring, RT, 24 h (iv) Heating, 140 °C, 4 h (chemical etching)	**[Cell membrane coating/Drug loading]** (i) HMPB, rtPA solution, stirring, 24 h (ii) Sonication in platelet membrane suspension solution, ice, 3 min, extrusion (iii) Mix with DPPC, DSPE-mPEG2000, cholesterol, $CHCl_3$, 55 °C, hydration	- Activating plasminogen conversion to plasmin to dissolve fibrin components in thrombus - Thrombus-specific targeting	~221 nm (square)	[92]

(*continued on next page*)

Table 1 (*continued*)

Synthesis strategy	Prussian Blue form	Synthesis condition (Reaction time, Temperature/Pressure)	Surface engineering condition	Engineering advantages	Size	Ref
	Se-HMPB	(i) PVP, $K_3[Fe(CN)_6]$, HCl, stirring, RT, 30 min (ii) 80 °C oven, 24 h (iii) PB, PVP, HCl, stirring, RT, 3 h (iv) Heating, 140 °C, 4 h (chemical etching)	**[Metal depositing]** (i) HMPB, Na_2SeO_3, DW, stirring, 30 min (ii) Ascorbic acid, RT, stirring, 3 h	- Performing GPx activity - Downgrading oxidative stress level in T cells and inhibiting differentiation	~145 nm (square)	[116]
Modified precipitation [MP]	PBNPs	(i) $FeCl_3$, citric acid, $K_4[Fe(CN)_6]$, water, stirring, RT, 5 min	[Bare Surface]	- Improving hydrophilicity without aggregation	~110 nm	[88]
	MPBZs	(i) PVP, $K_4[Fe(CN)_6]$, $MnCl_2$, trisodium citrate dihydrate, water, stirring (ii) PVP, $K_4[Fe(CN)_6]$•, water, stirring, 30 min (iii) Mix together, stirring, 1 h		- Improving hydrophilicity without aggregation - Targeting at inflamed sites using negative charge after oral administration	~60 nm (oblong)	[89]
Modified precipitation /Post-modification [MP]+[M]	PB/RBC	(i) $FeCl_3$•$6H_2O$, citric acid, $K_4[Fe(CN)_6]$, water, stirring, 60 °C, 30 min	**[Cell membrane coating]** (i) RBC membrane (ultrasonic/220 nm filtered), ultrasonication, 37 °C, 8 h incubation	- Prolonging material residence time in blood - Facilitating accumulation at lesion site	~74 nm (circle)	[90]
	Sim@ PMPB NC	(i) BSA, $K_4[Fe(CN)_6]$, water, stirring, RT, 30 min (ii) $MnCl_2$, BSA, stirring, RT, 30 min (iii) Mix together, stirring, RT, 25 h	**[Drug loading]** (i) Simvastatin, stirring, RT, 12 h	- Scavenging reactive oxygen species (ROS) - Mitigating inflammation - Lowering oxidized LDL internalization	~200 nm (square)	[84]
	PB-PFP@ PC	(i) $FeCl_3$•$6H_2O$, citric acid, stirring, 60 °C (ii) $K_4[Fe(CN)_6]$, same amount of citric acid, stirring, 60 °C, 1 min (iii) Stirring, RT, 30 min, dialysis	**[Peptide modification/Liposomal coating]** (i) Emulsifying with PLGA-PEG-CREKA, PVA, PFB, ultra-sonicating, 3 min, ice (ii) Emulsifying again by adding PVA, CH_2Cl_2 ultrasonicating, 3 min, ice (iii) Add isopropanol, stirring, 3 h, CH_2Cl_2 volatilization	- Destroying blood clots - Improving biocompatibility - ROS elimination for antithrombotic effect - Targeting fibrin - Photothermal therapeutic effect	~287 nm (circle)	[93]
	CPB–Ce6 NPs	(i) $FeCl_3$, citric acid, Stirring, 60 °C (ii) $K_4[Fe(CN)_6]$, water, stirring, 60 °C (iii) Mix, 60 °C, 30 min	**[Photosensitizer attachment]** (i) EDC•HCl, NHS, MES buffer, stirring, 30 min (ii) NH_2-Ce6, stirring, 12 h	- Performing MRSA killing activity by generating $^1O_2$	~150 nm (circle)	[91]
	PB NZs	(i) Chitosan, HCl, AcOH, RT, stirring, 24 h, filtration (ii) $K_3[Fe(CN)_6]$, CS solution, stirring, RT, 30 min (iii) Add $FeCl_2$ solution, stirring, RT, 1 h	**[Biopolymer coating]** (i) In situ reaction	- Improving biocompatibility and biodegradability - Low immunogenicity	4 nm	[95]
	RHPAzyme	(i) PVP, $K_3[Fe(CN)_6]$, HCl, stirring, RT, 2 h (ii) 80 °C oven incubation, 24 h (iii) PVP, PB, HCl, stirring, 140 °C, 4 h	**[Drug loading/Peptide labeling]** (i) Rapa, PB (10:1), EtOH, stirring, 24 h (ii) mPEG-COOH, EDC, NHS, water, ACPP, stirring, RT, 24 h (iii) Ultrafiltration (5 kDa), stirring, 12 h, (iv) PEG-ACPP, HMPB, (1:1 wt%), EtOH, stirring	- Ability to target lesion area	~240 nm (square)	[94]
Hydrothermal method [H]	HPBZs	(i) PVP, $Bi(NO_3)_3$, HCl, stirring (ii) PVP, $K_3[Fe(CN)_6]$, HCl, stirring (iii) Dropwise (ii) into (i), stirring, 3 h (iv) Incubation, 80 °C, 24 h	[Bare Surface]	n.r.	n.r.	[103]
Hydrothermal method/Post-	PBK NPs	(i) PVP, $K_3[Fe(CN)_6]$, HCl, stirring, RT, 30 min	**[Peptide modification]**	- Ability to target BBB - Binding to Aβ	163 nm (square)	[104]

(*continued on next page*)

Table 1 (*continued*)

Synthesis strategy	Prussian Blue form	Synthesis condition (Reaction time, Temperature/Pressure)	Surface engineering condition	Engineering advantages	Size	Ref
modification [H]+ [M]		(ii) 80 °C oven, 20 h	(i) Dispersed with PEI solution, stirring, RT, 2 h (ii) PB-PEI, reacted with sulfo-SMCC solution, stirring, 2 h (iii) add CKLVFFAED peptide solution, 4 °C, incubation overnight			
	PB@Lipo	(i) PVP + $K_3[Fe(CN)_6]$, $MnCl_2$, HCl, stirring, 80 °C, 24 h,	**[Liposomal coating]** (i) Mix hydrogenated soybean phospholipids, cholesterol, DSPE-PEG2000, chloroform, isopropyl ether, methanol (6:6:1) (ii) Add PB solution, shaking, 5 min, solvent evaporation at 45 °C	- Amphiphilic - Improving blood cell clearance - Improving biocompatibility, safety, and degradability - Great stability and solubility - Skin accumulation	100 nm (circle)	[105]
	KBP@KH hydrogel	(i) PVP + $K_3[Fe(CN)_6]$, HCl, stirring, RT, 30 min (ii) 80 °C oven, 20 h	**[Hydrogel engineering]** (i) KBP: PB, KGM, PB, PBS, stirring, 24 h Add BSA solution, stirring, 24 h (ii) BP: PB, BSA solution, sonication, RT, 24 h (iii) KH hydrogel: MPC, KGM, HACC, PBS, stirring, 80 °C (iv) Add PB, KBP, BP, freezing and thawing, −20 °C, six cycles	- Promoting angiogenesis - Enhancing cellular membrane permeability - Improving antioxidant capacity - Interacting with sulfur for preventing bacterial infection	250 nm (square)	[106]
	PB @MSCM	(i) PVP + $K_3[Fe(CN)_6]$, HCl, stirring, RT, 1 h (ii) 80 °C oven, 20 h	**[Cell membrane coating]** (i) MSCs membrane, ice-cold PBS, sonication, 2 min (ii) Add PB, sonication, 2 min	- Improving biocompatible surface properties - Enhancing injury site targeting	150 nm (square)	[107]
Micro-emulsifying [E]	PBNPs @PLEL	(i) Triton X-100, hexanol, cyclohexane, Mixng, RT (ii) Citric acid, $FeSO_4$ solution, stirring (iii) $K_3[Fe(CN)_6]$, citric acid, stirring (iv) Mix (i)–(iii), RT, 30 min, warming, 80 °C	**[Polymer coating]** (i) PDLLA-PEG-PDLLA synthesis: - PEG, 100 °C - Add D,L-lactide, $Sn(Oct)_2$, stirring, 140 °C, 12 h, argon (ii) Dissolve PDLLA-PEGPDLLA in PB microemulsion, shaking, 4 °C	- Improving biocompatibility - Mediating gradual sustained growth factors - PB delivery and sustained release - Injectable effect	71 nm (circle)	[110]

*n.r.: not reported.

safety and mediate the efficient production of high-quality PB that is suitable for large-scale applications by maintaining the desired physicochemical properties of the synthesized material. Recent studies have synthesized high-quality PB under low-temperature and low-pressure conditions, which is a deviation from the traditional requirements of hydrothermal synthesis [98]. Notably, Ye et al. have reported a template-free hydrothermal strategy, which uses bismuth nitrate as the key component [103]. In this study, PB was synthesized at a moderate reaction temperature of approximately 80 °C instead of the typical high-temperature conditions. As the synthesis of hollow PB typically requires a series of multi-step reactions, the inclusion of bismuth ions (Bi^{3+}) enables a streamlined one-pot synthesis process. In this approach, Bi^{3+} ions bind to PVP to form an intermediate complex (Bi^{3+}/$[Fe(CN)_6]^{3-}$/PVP). During the reaction, ferricyanide is decomposed by the action of a reducing agent while ionic competition promotes the growth of porous PB on the substrate surface. This method exhibits significant advantages such as ease of large-scale synthesis and simplified post-treatment processes.

Increasingly, hydrothermal synthetic strategies for the modulation of ROS levels for therapeutic purposes have incorporated surface engineering techniques to impart disease-specific functionalities. Song et al. used a strategy of coating PB with PEI to enhance its capacity to penetrate the BBB [104]. They conjugated peptides to PB surface to achieve selective disaggregation of the particle in regions affected by Alzheimer's disease (AD). This strategy highlights the targeted design approach for addressing neurological diseases.

Xie et al. implemented a novel synthetic methodology for embedding highly uniform PBNPs (approximately 100 nm), which were synthesized *via* the hydrothermal method in a lipid matrix comprising soybean phospholipids, cholesterol, and biotinylated PEG2000, for application in wound care of inflammatory diseases [105]. Using a reverse-phase evaporation method, they significantly enhanced the intrinsic biocompatibility of PB by forming a liposome. Additional functionalization further amplified the anti-inflammatory properties of the PBNPs, which accelerated wound healing in inflammatory settings.

In 2024, Tang et al. developed a PB combined with hydrogel to address the elevated ROS levels associated with diabetic foot ulcers (DFU). Their approach involved the integration of bovine serum albumin and konjac glucomannan (KGM) derived from corn with PB synthesized *via* the hydrothermal method [106]. The resulting PB hydrogel composite exhibited highly improved cellular uptake and antioxidant activity. This study has demonstrated the effectiveness of this therapeutic strategy.

Zhang et al. aimed to alleviate the damage instigated by radiation-induced hematopoietic injury using a biomimetic cell membrane camouflage approach [107]. They enveloped PBNPs with mesenchymal stem cell (MSC) membranes. This strategy optimized bone marrow treatment by increasing the extensive proliferative potential and low immunogenicity of MSCs.

In summary, these sophisticated strategies accentuate the potential of PBNPs in diverse biomedical applications and highlight their adaptability and promising role as multifunctional therapeutic agents.

4.3. Microemulsion method

The microemulsion method for PB synthesis comprises two distinct steps (Fig. 4c). Initially, a homogeneous emulsion is generated by incorporating surfactants into an aqueous medium comprising two precursors: metallic ions and coordinating ligands. Subsequently, solid-phase PB is excessively precipitated in the second step [108,109]. This method was pioneered by Xu et al. and has significantly advanced the synthesis of various inorganic nanoparticles because of its precise control over nucleation and particle growth [110]. As this is a thermodynamically stable system, it does not require any external energy input, which enables it efficient and straightforward synthesis under minimal energy conditions.

This method was first applied in 1999 for the synthesis of PB analogs based on copper hexacyanoferrate (III) [111,112]. Although the initial study did not achieve well-defined particles, it instigated extensive research in this field. The surfactants that are most frequently used in this method include bis(2-ethylhexyl) sulfosuccinate (AOT), cetyltrimethylammonium (CTMA), and neutral surfactants such as Brij and IGEPAL [113,114]. The PB particle size can be meticulously regulated by adjusting the ratio and concentration of the solvent and surfactant, which enables versatile particle design. PB synthesized through this microemulsion technique is distinguished by its tunable size, structural morphology, and excellent dispersive attributes. However, its reliance on surfactants during the synthesis process may affect the PB surface characteristics, which could potentially introduce impurities. This is a notable limitation that requires further consideration.

Xu et al. used this technique to synthesize PB for applications in diabetic wound management [110]. They used a combination of Triton X-100, hexanol, and cyclohexane in two discrete batches for the synthesis. The initial batch incorporated citric acid and $FeSO_4$, whereas the subsequent batch used citric acid and $K_3[Fe(CN)_6]$ to form microemulsions, from which PB was harvested. To tailor PB for its specific application, they developed a PB hydrogel using thermosensitive polymers to facilitate controlled PB release within the wound environment.

PB produced through the representative synthetic process can undergo a chemical etching process to expand its applicability. This process enables the formation of porous hollow PB or further contributes to the reconstruction of Prussian blue analogs (PBAs) (Fig. 4d). The basic reaction process for understanding PB synthesis is schematically summarized in Fig. 4e, illustrating how nuclei, formed through ion exchange of reagents used in the synthesis, develop into specific sizes and morphologies during the aging process.

Thus, various strategies used for upgrading ROS scavenging capabilities are presented in this review to aid in the design of disease-specific PB systems. We hope that these reported advancements provide critical insights for forthcoming research endeavors and promote the development of innovative PB-based therapeutic approaches.

5. Biotherapeutic applications of PB in ROS-related diseases

ROS extensively contribute to the occurrence of diseases and play significant roles in disease pathologies (Table 2). ROS balance is disrupted in most disease lesion, which leads to persistently elevated ROS levels that exacerbate pathological conditions. Consequently, several therapeutic strategies incorporate methods that simultaneously treat the disease while modulating ROS levels. In this section, we have categorized ROS-related disease into neurological, cardiac/vascular, inflammatory, and other diseases and have elucidated the role of ROS in the pathology of each disease type. PB-based nanomaterials show great potential as efficient therapeutic agents in the treatment of these diseases through their notable ROS scavenging capability.

5.1. Neurological diseases

Neurological diseases are commonly defined by an extensive set of

Table 2
Role of ROS in various diseases.

Category	Diseases	Role of ROS	Ref
Neurological diseases	Alzheimer's diseases Parkinson's diseases Stroke	(+) Synaptic plasticity (+) Maturation of neurons (+) Activation of transcription factors (−) Neuronal toxicity (−) Apoptosis of neurons (−) Cerebral ischemia (−) Dysregulation in microglia (−) Glutamate excitatory toxicity (−) Iron homeostasis	[79,80,82,83,88,90,104]
Cardiovascular diseases	Atherosclerosis Myocardial infarct Ischemia-Reperfusion Injury Thrombosis Hypertension Retinal dysfunction Pneumoconiosis Vascular injury Acute respiratory distress syndrome	(+) Maintaining normal vascular physiology (+) Wound repair (+) Relaxation of cerebral arteries (−) Endothelial dysfunction (−) Vascular abnormalities (−) Impairment of DNA, proteins, and lipids (−) Reducing nitric oxide (NO) availability (−) Promoting arterial hypertension (−) Reducing vasoconstriction (−) Heart cell dysfunction	[75,76,84–86,92,93,115]
Inflammatory diseases	Rheumatoid arthritis Inflammatory bowel disease Diabetic wound Periodontitis Tendinopathy Bronchitis Emphysema Bone-related diseases (Osteoporosis)	(+) Supporting immune system (+) Killing Macrophages (+) NF-κB activation (+) Inflammasome signaling (−) Endothelial dysfunction (−) DNA damages (−) Genomic instability (−) Accelerating neoplasm (−) Insulin resistance (+) Bone remodeling (+) Maintaining mineral tissue homeostasis (−) Poor skeletal healing (−) Inhibiting osteoblast differentiation (−) Inducing apoptosis of osteocytes and osteoblasts (−) Reducing bone matrix deposition (−) Shifting balance towards bone loss	[81,89,91,103,105–107,110,116]
Other diseases	Organ failure (Liver, Renal)	(+) Respiratory plasticity (+) Sensory plasticity (−) Inflammation (−) Tissue injury	[78,95]

(continued on next page)

Table 2 (*continued*)

Category	Diseases	Role of ROS	Ref
	Cancer	(−) Organ dysfunction (+) Impairing tumorigenesis (+) Cancer cell apoptosis (−) Promoting metastasis (−) Initiating and assisting tumor progression (−) Facilitating pro-tumorigenic signaling (−) Radio-resistance (−) Carcinogenesis	[30]

*(+): advantages, (−) disadvantages.

pathophysiological conditions that emerge in the cerebral regions, spinal cord, and peripheral nerve structures [117]. The WHO has reported that these neurological conditions rank among the foremost contributors to both disability and mortality on a global scale with cerebrovascular accidents identified as the second primary cause of death internationally owing to neuronal loss, accumulation of protein and aggregation, neuronal inflammation, and ROS-induced oxidative stress [118]. Particularly, ROS exerts a more significant impact on the nervous system than on other physiological tissues, leading to glial cell impairment, cerebral lipid peroxidation, and alterations in neurotransmitter concentrations. However, despite the shared pathological features among various neurological diseases, each disorder possesses unique attributes and distinct trajectories of progression. The most well-supported hypothesis may be observed in the framework of AD, particularly in the mechanisms underlying the aggregation of beta-amyloid (Aβ) proteins and hyperphosphorylation of tau proteins, which results in the formation of tau tangles. PD exhibits a loss of dopamine-producing neurons, and stroke involves acute blood flow disruption. Therefore, comprehending the underlying mechanisms associated with each pathological condition is imperative to formulate efficacious and precisely directed therapeutic interventions. Ultimately, despite the different pathological inducing factors, ROS play significant roles in promoting diseases; hence, approaches based on ROS scavenging *via* PB are being actively studied. We have summarized the therapeutic effects of PB-based nanomaterials in the context of each neurological disease in Table 3.

5.1.1. Alzheimer's disease (AD)

In the AD framework, oxidative stress significantly impacts the underlying cellular metabolic mechanisms and neuronal operations, which promote AD progression. Aggregation and accumulation of amyloid-beta precursor protein onto plaques and phosphorylated tau tangles are the major stressors that are hallmark features of AD. This phenomenon triggers a neuronal inflammatory response, which instigates mitochondrial dysfunction before ultimately culminating in neuronal apoptosis (Fig. 6a) [119]. Joanna et al. used PB as a therapeutic intervention in AD owing to its efficacy in scavenging and suppressing ROS levels [88]. PBNP application significantly attenuated the characteristic Aβ fibril formation and concurrently restored regular amyloid fibrillation. Additionally, it showed chelating efficacy towards copper ions, which are implicated in the mediation of Aβ-bound Cu^{2+} formation that leads to the generation of neurotoxic ROS. Through this mechanism, PBNPs produce a 60 % reduction in Cu^{2+} levels and perform a protective function in mitigating membrane disruption.

In a separate study, Li et al. functionalized PB nanoparticles with red blood cells (RBCs) to improve translocation across the BBB [90]. The PB/RBC nanocomposite significantly reduced Cu^{2+}-induced Aβ aggregation, and NIR irradiation successfully eliminated Aβ fibrils. Thereby, this intervention reduced neuroinflammation and addressed mitochondrial impairments. In a model of AD, PB/RBC enhanced memory performance and cognitive deficits. Song et al. used a different type of coating technique using functional peptides to enhance BBB permeability and PB efficacy (Fig. 6b–d) [104]. They used K-peptide, which is an amino acid sequence derived from Aβ protein. The PBK nanoparticles exhibited superior binding affinity for Aβ and effectively induced Aβ plaque disintegration. Furthermore, this therapeutic effect was significantly amplified when combined with NIR irradiation. Within the AD microenvironment, PBK nanoparticles showed notable antioxidant capabilities by efficiently scavenging ROS. Thus, PBK nanoparticles alleviated mitochondrial dysfunction and cellular apoptosis and protected neuronal cells from AD-associated damage. In murine models of AD, the cohort receiving PBK nanoparticles in combination with NIR therapy exhibited substantial enhancement in anxiety-like behaviors and spatial learning capacities.

5.1.2. Parkinson's disease (PD)

PD has been recognized as the second most common neuronal disease. It is caused by dopaminergic neuron degeneration. Despite the insufficient clarification of the pathophysiological mechanisms that govern PD, ROS has been widely recognized to perform a crucial function in PD pathogenesis. Owing to the degeneration of dopaminergic neurons, ROS levels increase excessively, which trigger pyroptosis and improper α-synuclein folding [120]. Furthermore, excessive ROS mediate the nucleotide-binding domain and leucine-rich repeat family pyrin domain containing 3 (NLRP3) inflammasome, which plays a key role in PD [121]. The NLRP3 inflammasome assembles in the microglia and initiates caspase-1 activation, which induces proinflammatory responses and pyroptosis. This interplay among these processes generates a detrimental cycle that advances PD (Fig. 7a). PB possesses protective properties against the apoptosis of dopaminergic neurons and is therefore a potential therapeutic agent for PD. Ma et al. demonstrated the effectiveness of PB nanozyme (named PBzyme) as a robust antagonist of pyroptosis; thus, PBzyme alleviated PD symptoms (Fig. 7b–d) [80]. Owing to its notable capacity for ROS scavenging, PBzyme proficiently reduces mitochondrial ROS concentrations and obstructs NLRP3 inflammasome activation within microglial cells, which are pivotal mediators in the etiology of various diseases. This intervention limits microglial pyroptosis and averts the death of dopaminergic neurons. In an MPTP-induced PD mouse model, PBzyme administration *via* intra-cerebroventricular injection significantly ameliorated motor deficits.

5.1.3. Stroke

Stroke is characterized as an abrupt cessation of cerebral blood flow because of localized occlusion within the brain and resulting in neurocognitive deficits such as dementia and depression [122]. Upon the restoration of blood flow during the reperfusion phase, consequential overproduction of ROS occurs, which causes mitochondrial dysfunction, neuronal inflammation, and apoptosis (Fig. 8a). On the other side, ROS induce the activation of microglial cells, which are resident immune cells of the brain tissue that protect it by eliminating harmful substances [123]. However, the persistence of ROS leads to overproduction of cytotoxic factors and potential destruction of the surrounding neural tissue. Thus, ROS are pivotal contributors to the pathophysiological progression of stroke, whereas PB exhibits neuroprotective properties by mitigating inflammatory responses in stroke-affected neuronal cells. Liu et al. showed that PBzyme exerted neuroprotective effect by eliciting notable ROS scavenging efficacy both *in vitro* and *in vivo*, which helped inhibit inflammatory response by downregulating pro-inflammatory cytokines [79]. Moreover, it promoted the polarization of microglia towards the M2 phenotype. In IRI model mice, PBzyme effectively inhibited caspase-3 protein expression, which induced anti-apoptotic effects.

Additionally, it aids in the recuperation of neurological function by enhancing cognitive abilities. Zhao et al. engineered dopamine-enveloped PB (PB@PDA) nanoparticles for effective localization in

Table 3
Therapeutic effect of PB in neurological disease.

Diseases	Prussian Blue forms	Type of ROS scavenging	Target scavenging route	ROS scavenging efficacy/ Administration	Therapeutic effects	Ref
Alzheimer's disease (AD)	PBNPs	POD-like activity	Inhibition of Cu^{2+} induced- Aβ aggregation	[In vitro] Conc. 10 μM - Aβ40 aggregation inhibition: ~16.2 % - Aβ40 aggregation inhibition: ~2.4 % (under Cu^{2+}/ROS in bacterial cells)	+ Capturing Cu^{2+} ions, partially restoring normal Aβ fibrillation + Preventing the formation of highly toxic Cu^{2+}-containing oligomeric species	[88]
	PB/RBC	SOD, CAT, POD-like activity	Inhibition of Cu^{2+} induced-Aβ aggregation	[In vitro] Conc. 200 μg/mL - •OH scavenging <70 % - SOD inhibition: ~38 % Conc. 50 μg/mL, - H_2O_2 inhibition: ~90 % [IV injection] - Dose: 0.2 mg/mL, injected every 3 days (for 4 weeks)	+ Preventing the formation of highly toxic Cu^{2+}-containing oligomeric species + Inhibiting neurotoxicity of Aβ aggregates. + Improving memory function and cognitive dysfunction	[90]
	PBK NPs	SOD, CAT, POD-like activity	Inhibition of Aβ aggregation	[In vitro] Conc. 100 μg/mL - $O_2^{\bullet-}$ inhibition: <80 % - •OH scavenging <70 % - O_2 generation: 22.5 mg/L (100 μL of 1 % H_2O_2) [IV injection] - Dose: 2 mg/kg, injected every 3 days (for 30 days)	+ Neuroprotective role against A*β*-and ROS-triggered neurotoxicity + Regulating Aβ deposition + Relieving neuroinflammation + Delaying AD progression by protecting neurons	[104]
Parkinson's disease (PD)	PBzyme	SOD, CAT, POD-like activity	Inhibition of NLRP 3 inflammasome	[In vitro] Conc. 25 ppm - $O_2^{\bullet-}$ inhibition: <47 % - •OH scavenging <47 % - H_2O_2 inhibition: <14 % [ICV injection] - Dose: 3 μL, (1 mg/mL) injected 24 h before MPTP treatment	+ Protecting microglia and neurons + Alleviating motor deficits + Attenuating mitochondrial membrane potential damage + Reducing dopaminergic degeneration and neuroinflammation	[80]
Stroke	PBzyme	SOD, CAT-like activity	Promotion of M2 type microglia	[In vitro] Conc. 10 μg/mL - SOD inhibition: ~80 % - O_2 generation: 2.5 mg/L (1.5 M H_2O_2 decompose) [IV injection] - Dose: 20 mg/kg, injected for 1 h after the thrombus was removed	+ Inhibition of macrophages activation + Release of inflammatory factors in the brain + Promoting M2 polarization + Promoting neuronal recovery + Reducing brain tissue loss	[79]
	PB@PDA	POD-like activity	Protection of mitochondrial dysfunction	[In vitro] Conc. n.r. - oxTMB generation: ~1.4-fold increment (650 nm) [IC injection] - Dose: 20 mg/kg, injected at 2 h after HI injury	+ Increasing oxidative defenses + Inhibiting neuronal apoptosis at early phase + Decreasing glial activation/pro-inflammatory cytokine expression + Inducing synaptic modifications + Improving neurobehavioral impairment + Facilitating motor function recovery	[83]
	MPBzyme@NCM	SOD, CAT, POD-like activity	Promotion of M2 type microglia	[In vitro] Conc. 100 ppm - •OH, •OOH, H_2O_2 < 50 % - lower SOD/CAT activity than that of natural SOD/CAT [IV injection] - Dose: 20 mg/kg, injected at 2 h after suture extraction	+ promoting proliferation of neuronal precursors and neural stem cells + inhibiting M1 responses + facilitating M2 responses in microglia + regulating indirect neuron repair	[82]

stroke-affected regions to provide synergistic antioxidant effect [83]. The introduction of PB@PDA nanoparticles in a neonatal hypoxia-ischemia (HI) model resulted in decreased neuronal cell death within the brain infarct region and significant accumulation within the brain. Thus, both short- and long-term stroke-associated behaviors were notably relieved. Feng et al. incorporated mesoporous PB with neutrophil-like cell membranes to improve penetration probability into the cerebral tissue (Fig. 8b–e) [82]. Neutrophils respond to the deleterious brain microenvironment by engaging with adhesion molecules in inflamed regions; this enables MPBzyme@NCM to target damaged neuronal cells through non-invasive delivery. The MPBzyme@NCM showed therapeutic efficacy in stroke models by promoting the M2 polarization of microglia and facilitating neurogenesis.

5.2. Cardiovascular diseases (CVD)

Atherosclerosis (AS), Thrombosis (TB), and Ischemia reperfusion injury (IRI) represent prevalent vascular pathologies that exhibit significant interconnections through analogous pathogenic mechanisms [124]. Occlusive thrombus that forms in the coronary artery leads to the formation of cardiac ischemic infarction [125]. AS is caused by lipid accumulation, inflammation, and damaged endothelium. It is the primary underlying mechanism that contributes to cardiac disease progression [126]. This condition accelerates plaque destabilization, which increases the likelihood of occlusive thrombus formation [127]. Thus, the thrombus may trigger IRI onset. ROS-induced oxidative stress is deeply associated with progression of cardiac diseases, which elicits inflammatory responses and mitochondrial dysfunction. Consequently,

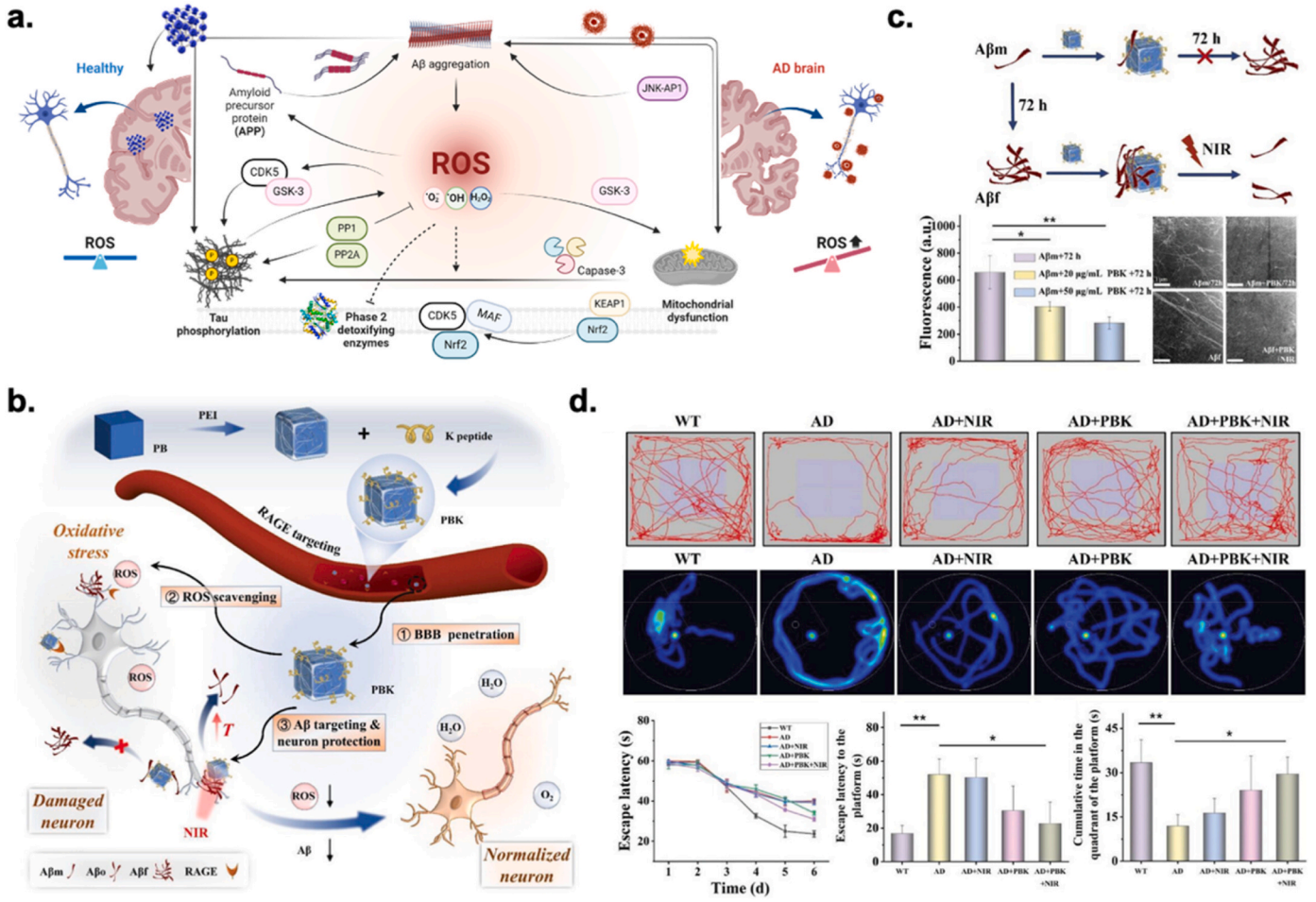

Fig. 6. (a) Role of ROS in Alzheimer's Disease (AD) pathology and progression. (b) Schematic of Prussian Blue K-peptide nanoparticles (PBK NPs) enable AD treatment by inhibiting Aβ fibrillation. (c) Influence of PBK NP treatment on Aβ fibrillation. (d) Evaluation of effect of PBK NPs on anxiety-like behavior and spatial learning abilities in AD model mice. Reprinted with permission [104], Copyright 2023, Wiley.

antioxidant therapy using PB is considered a promising therapeutic strategy for the management of vascular diseases. We have compiled a summary of the therapeutic effects of PB-based nanomaterials in various cardiac and vascular diseases in Table 4.

5.2.1. *Atherosclerosis (AS)*

Oxidized low-density lipoprotein (oxi-LDL) is a principal contributor to AS pathophysiology. The accumulation of oxi-LDL attracts macrophages, which subsequently results in foam cell formation. The aggregation of foam cells promotes inflammatory cytokines and recruitment of vascular smooth muscle cells (VSMCs), which eventually leads to plaque development within the arterial wall. ROS contribute to overall pathogenesis in various diseases by exacerbating oxi-LDL levels, which destabilizes plaques and leads to precipitating plaque ruptures. Furthermore, they induce thrombi formation, which amplifies the risk of myocardial infarction or cerebrovascular accident (Fig. 9a) [128]. PB not only prevents cholesterol oxidation but also regulates macrophage activation and by extension the secretion of inflammatory cytokines.

In addition to its function as a ROS scavenger, Chen et al. additionally used PB as a photoacoustic agent for the therapeutic intervention of AS [75]. n-PBEs exhibit considerable NIR absorption; hence, they function as imaging agents for plaque detection. In conjunction with their imaging efficacy in AS, n-PBEs showed therapeutic potential by attenuating ROS levels, decreasing macrophage apoptosis, and reducing oxi-LDL level, thereby inhibiting foam cell formation. Zhang et al. formulated a therapeutic agent by encapsulating simvastatin (Sim), which is an antioxidant pharmacological compound, within manganese-substituted PB (Fig. 9b–e) [86]. This formulation was engineered to facilitate the release of Mn^{2+} *via* reactions with H_2O_2 in inflammatory lesions to enable the visualization of atherosclerotic plaques. Consequently, the Sim@PMPB nanocomplex exhibited theragnostic capabilities as it enhanced antioxidant effects and improved diagnostic accuracy by augmenting T1-MRI contrast.

Furthermore, Zhou et al. innovatively engineered a PB form by incorporating artemisinin (ART) and procyanidins (PC) and coating the construct with macrophage and red blood cell membranes [84]. The simultaneous loading of the two pharmacological agents effectively modulated the fluxion of lipids and cholesterol. The cell membrane coatings enhanced immune evasion and facilitated plaque targeting. Thus, HA-M@PB@(PC + ART) nanoparticles exhibited significant anti-atherosclerotic effects *in vivo* in $ApoE^{-/-}$ mouse models.

5.2.2. *Thrombosis (TB)*

TB is an AS complication, accompanied by platelet aggregation and establishment of a fibrin matrix. Platelet is the primary component of thrombosis and is activated by ROS [92]. Disrupted blood flow activates endothelial cells to incite ROS formation, which promotes platelet–leukocyte aggregation. Similarly, leukocytes modulate the expression of mononuclear cells through ROS, which signifies the pivotal role of oxidative stress in thrombosis and atherogenesis. This mechanism initiates a sequential series of coagulation events that involve mast cells and VSMCs, ultimately leading to thrombus formation. Then, the thrombus entraps erythrocytes and platelets in fibrin networks. This cascade reaction exacerbates the vascular microenvironment and

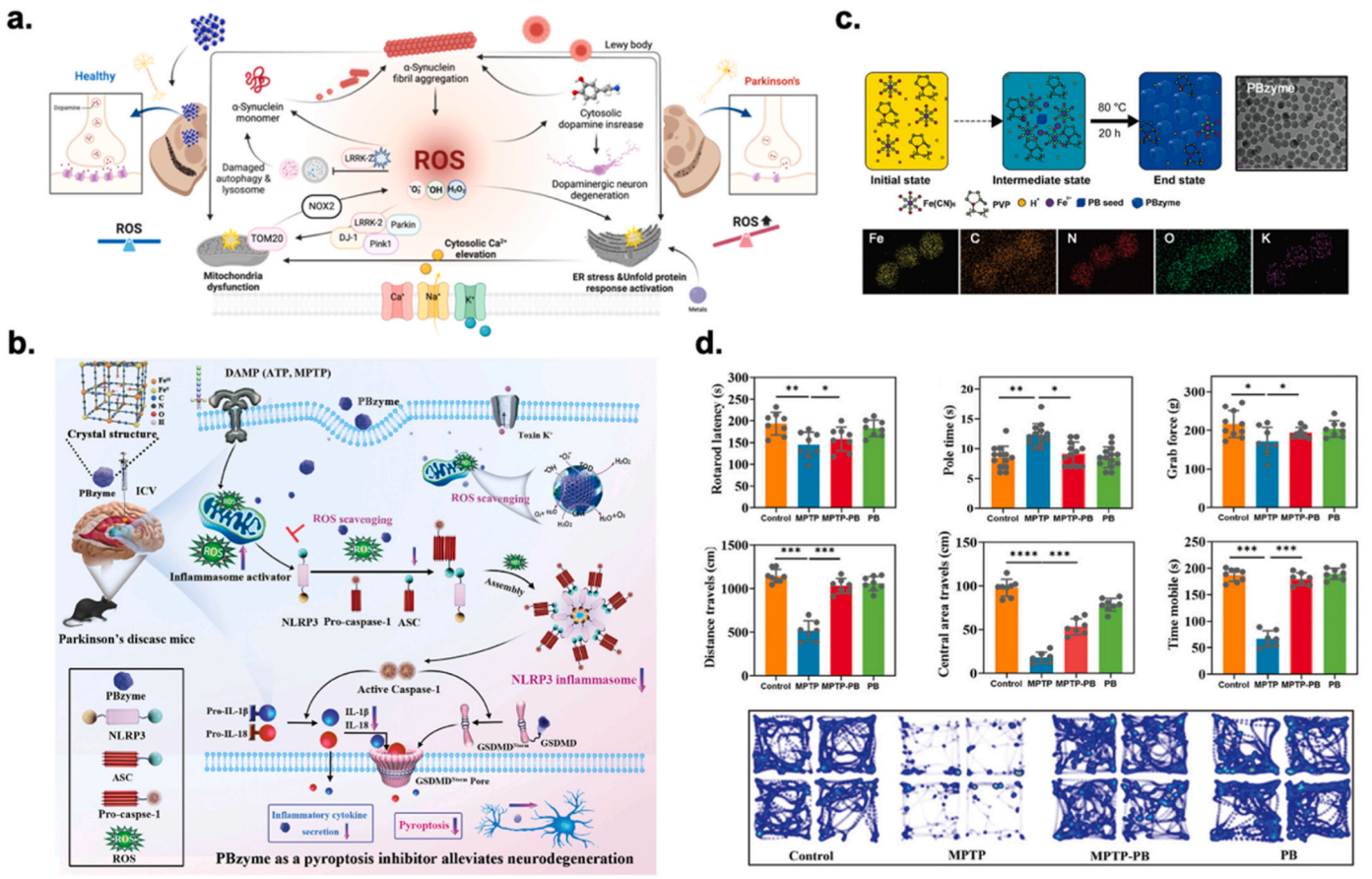

Fig. 7. (a) Role of ROS in Parkinson's Disease (PD) pathology and progression. (b) Schematic of mechanism underlying PB nanozyme (PBzyme) activity for PD treatment. (c) Synthesis, methodology, and transmission electron microscopy (TEM) images of PBzyme. (d) PBzyme attenuates motor deficits in the MPTP-induced PD mouse model *via* ICV administration. Reprinted with permission [80], Copyright 2022, Wiley.

contributes to increased oxidative stress (Fig. 10a). PB diminishes thrombus formation by obstructing platelet activation and aggregation. Additionally, PB influences the enhancement of endothelial cell functionality by augmenting the antithrombotic attributes of the vascular endothelium. Zhang et al. reported the efficacy of PB as an antithrombotic agent that synergistically integrates antioxidant properties with direct thrombolytic capabilities (Fig. 10b–d) [93]. They designed a drug-free antithrombotic therapeutic approach by incorporating photothermal therapy in conjunction with optical droplet vaporization (ODV) facilitated by perfluoropentane (PFP) modification. The PB-PFP@PC nanodroplets effectively dismantled the fibrin network architecture and simultaneously supplied oxygen to enhance ultrasound-mediated monitoring. Moreover, the fibrin-targeting efficacy conferred by the CREKA peptide facilitated enhanced accumulation at the thrombus site. Thus, in prolonged thrombolysis assessments, the PB-PFP@PC formulation showed a thrombus dissolution rate of 74.4 %. In a related study, PB was engineered with platelets to act as a drug delivery vehicle that specifically targeted thrombi [129]. The HMPB-rtPA@PM formulation exhibited specificity in targeting thrombi and reduced ROS levels and platelet aggregation. Thus, it effectively delayed thrombi progression through a dual mechanism involving PTT and pharmacological interventions in a Black tail thrombus mice model of fibrinolysis.

5.2.3. *Ischemia-reperfusion injury (IRI)*

IRI occurs after a transient obstruction of blood flow, followed by its restoration [130]. The major proportion of ROS is generated post-reperfusion and is associated with intricate metabolic processes. During the reperfusion phase, the abrupt reintroduction of oxygenated blood into a previously hypoxic environment characterized by acidic pH triggers mitochondrial dysfunction, cellular apoptosis, and activation of inflammatory pathways. This sequential cascade results in irreversible cellular damage, which may result in pronounced organ dysfunction. Therefore, rapid and effective ROS scavenging is imperative to mitigate damage during the reperfusion phase (Fig. 11a). In this context, PB may be used as a potential therapeutic agent against IRI owing to its excellent antioxidant properties and anti-inflammatory effects.

Huang et al. have elucidated the protective effects of PB in the context of hepatic IRI. They found that PB reduced ROS levels in hepatocytes and macrophages, inhibited cellular apoptosis, and promoted M2 polarization, which mitigated inflammatory responses [115]. Liu et al. have studied the therapeutic efficacy of PB-based nanoparticles in myocardial IRI [85] using the drug-loaded nanoplatform DSS/PB@BSP, which effectively facilitated the circulation of therapeutic agents-carrying monocytes. This further enhanced M2 polarization in inflamed lesions. Moreover, through sustained drug release and induction of anti-inflammatory M2-type macrophages, the platform exhibited notable efficacy in repairing cardiac function in a mouse model of MI/RI. Another study used PBzyme to alleviate IRI and showed enhanced survival rate for skin flaps (Fig. 11b–e) [76]. PBzyme mitigated inflammatory responses by scavenging ROS and attenuating inflammatory cytokine secretion, which augmented the rates of cellular viability and suppressed necroptosis. Furthermore, it stimulated angiogenesis by elevating VEGFA expression. Thus, the IRI model showed significantly augmented survival rate for skin flaps from 37.21 % to 79.61 %.

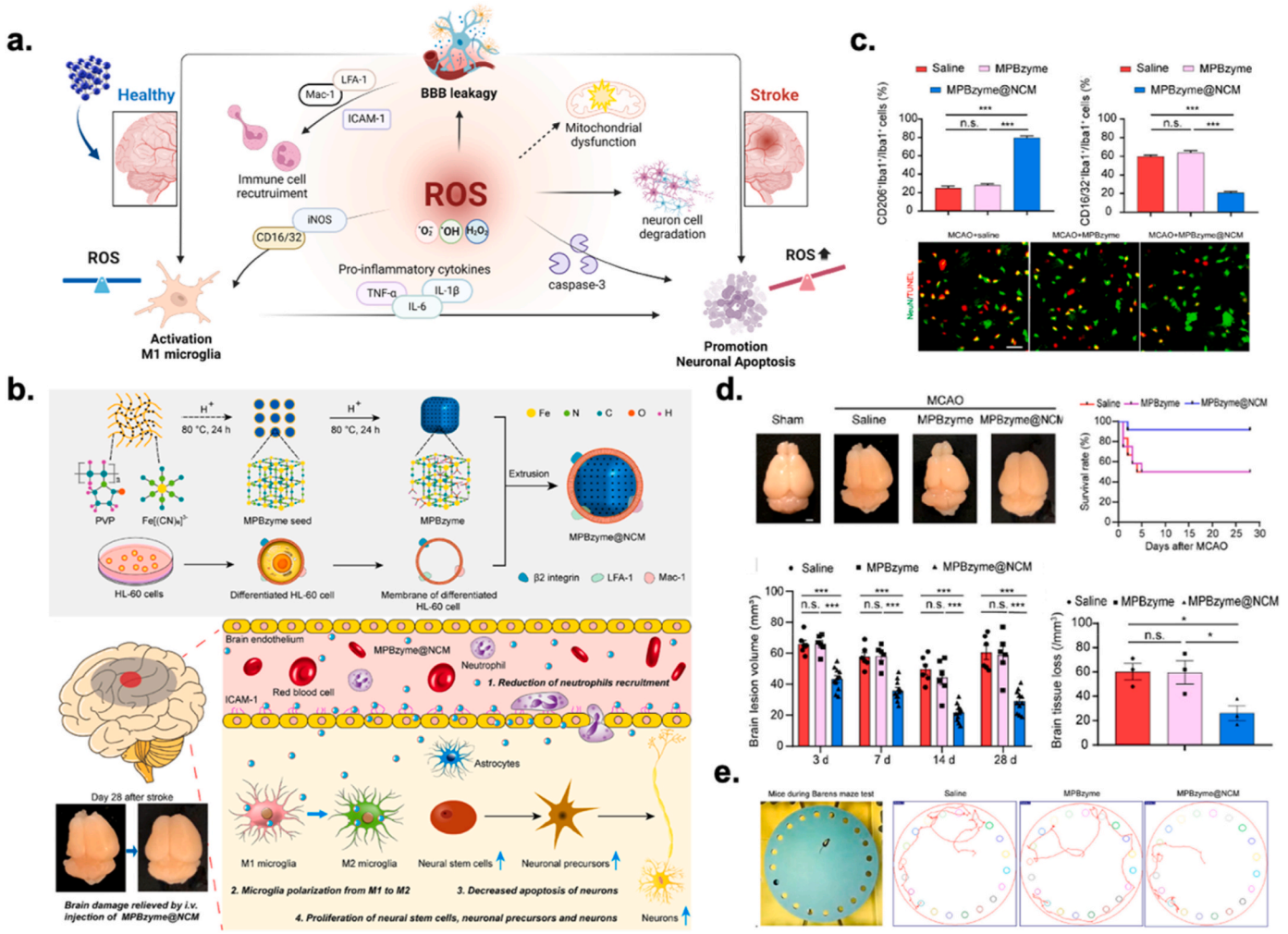

Fig. 8. (a) Role of ROS in stroke pathology and progression. (b) Schematic of MPBzyme@NCM synthesis and therapy for ischemic stroke. (c) Promotion of microglia polarization to M2 by MPBzyme@NCM. (d) MPBzyme@NCM alleviated long-term brain tissue damage and improved long-term survival rate after stroke *in vivo*. (e) *In vivo* long-term neurological functional recovery after stroke following MPBzyme@NCM treatment [82]. Copyright 2021, American Chemical Society.

5.3. *Inflammatory disease (ID)*

Inflammation is the defense system of the body to restore damaged tissue and remove antigens from inflamed lesions. The underlying mechanism involves the generation of ROS by the activated immune cells to target pathogens and enhance immune responses through the release of signaling molecules [131]. Nevertheless, chronic and persistent inflammation induces an imbalance in the antioxidant system, which results in autoimmune reactions that compromise normal cells and tissues. This is known as inflammatory diseases (ID). Moreover, excessive ROS production stimulates pro-inflammatory cytokines that severely exacerbate inflammatory responses [132]. The therapeutic effects of PB-based nanomaterials in various inflammatory diseases have been presented in Table 5.

5.3.1. *Wound healing (WH)*

The occurrence of wounds leads to an immediate initiation of inflammatory response and recruitment of macrophages and neutrophils to the inflamed lesion. The accumulated immune cells generate ROS, which are integral in negating infection, combating pathogens, and concurrently aiding in the clearance of necrotic tissues. During the proliferation phase, ROS facilitate angiogenesis and migration of fibroblasts, which are critical for tissue regeneration [133]. However, excessively prolonged inflammatory responses may inhibit and prolong the healing process following the proliferation phase. Excessive ROS levels directly degrade the extracellular matrix (ECM) collagen by upregulating matrix metalloproteinases (MMPs). Consequently, maintaining optimal ROS levels is imperative for an efficient wound-healing process (Fig. 12a) [134]. We have presented several PB-based therapeutics that may enhance the wound-healing process by protecting fibroblasts and endothelial cells from oxidative stress to preserve ECM integrity.

Xie et al. reported a novel liposome-encapsulated PB (PB@Lipo) formulation, which notably improved the efficacy of the skin wound healing process [105]. The incorporation of liposomes significantly improved PB dispersal and stability. Moreover, it exhibited notable antioxidant properties, which facilitated macrophages differentiation into the M2 phenotype, resulting in the induction of anti-inflammatory responses. PB@Lipo administration reduced the wound area to 2 % of the initial defect, accompanied by the upregulation of collagen types 1 and 2, which fostered collagen fiber synthesis. In another study, Xu et al. examined the implications of integrating PBNPs into a thermosensitive hydrogel for the healing of diabetic wounds (Fig. 12b–e) [110]. PBNPs@PLEL restored the functionality of the NRF2/HO-1 signaling pathway, which initiated antioxidant responses. Moreover, it exerted protective effects on mitochondrial functionality by preserving membrane potential, mitigating calcium overload, and reinstating ATP synthesis within mitochondria. Subsequently, it reduced the expression of pro-inflammatory cytokines such as IL-6 and TNF-α and promoted angiogenesis by upregulating CD31 and α-SMA expression. It

Table 4
Therapeutic effect of PB in cardiovascular diseases.

Diseases	Prussian Blue forms	Type of ROS scavenging	Target scavenging route	ROS scavenging efficacy/ Administration	Therapeutic effects	Ref
Atherosclerosis (AS)	HA-M@PB@ (PC + ART)	SOD-like activity	Modulation of lipid influx and cholesterol efflux	[In vitro] Conc. 35 μg/mL - DCFH-DA <70 % (RAW264.7 cells, ROS induced by 500 ng/mL LPS) [IV injection] - Dose: 5 mg/kg, injected twice per week (for 8 weeks)	+ Significant scavenging effect on ROS and NO + Inhibiting NF-κB/NLRP3 pathway with suppression of lipid influx + reducing uptake and internalization of oxLDL + Promoting cholesterol efflux	[84]
	Sim@ PMPB NC	SOD, CAT, POD-like activity	Suppression of Macrophage infiltration and oxi-LDL internalization	[In vitro] Conc. 200 μg/mL - H_2O_2 inhibition: <0.16 % - •OH scavenging <60 % Conc. 500 μg/mL - DPPH inhibition: <25 % [IV injection] - Dose: 20 mg/kg, injected once a week (for 4 months)	+ Scavenging excessive ROS including free radicals and H_2O_2 + Decreasing pro-inflammatory cytokine secretion + Holding up macrophage infiltration + Reducing VSMC proliferation and collagen/MMP-9 expression + Anti-atherosclerosis activity	[86]
	n-PBEs	SOD, CAT, POD-like activity	Suppression of Macrophage infiltration and oxi-LDL internalization	[In vitro] Conc. 200 μg/mL - H_2O_2 inhibition: <50 % - $O_2^{\bullet-}$ inhibition: <65 % - •DPPH inhibition: <35 % - •ABTS inhibition: <50 % [IV injection] - Dose: 2.5 mg/kg, (for 10 weeks)	+ Downregulating ROS level + Inhibiting macrophages, apoptosis, and foam cell formation + Reducing oxLDL internalization in atherosclerotic plaque areas and AS development	[75]
Ischemia–reperfusion injury (IRI)	PBzyme	SOD, CAT, POD-like activity	Inhibition of necroptosis	[In vitro] Conc. 40 μg/mL - H_2O_2 inhibition: <25 % - $O_2^{\bullet-}$ inhibition: <46.4 % - •OH inhibition: <50 % Conc. 2.4 μg/mL - O_2 generation: 1.74 mg/L (1.2 M H_2O_2 decompose) [ID injection] - Dose: 1 mL, 2 h before surgery (for 6 h)	+ Promoting survival of transplanted skin flap + Excellent ROS-scavenging ability + Reducing apoptosis and mortality + Maintaining cell functions and tube formation + Inhibiting inflammation by regulating PPAR-γ/NF-κB signaling pathway	[76]
	PB Scavengers	SOD, CAT, POD-like activity	Inhibition of neutrophil infiltration, promotion of M2 macrophage	[In vitro] Conc. 50 μg/mL - •OH inhibition: <56.6 % - O_2 generation: 32.5 mg/L [IP injection] - Dose: 1 mg/kg, Injected 24 h before IRI	+ Protecting liver tissue by scavenging ROS + Reducing neutrophil infiltration + Promoting macrophage M2 polarization + Reducing oxidative stress in primary hepatocytes, restoring cell viability + Reducing inflammation	[115]
	DSS/PB@BSP	n.r.	Promotion of M2 macrophage	[In vitro] Conc. 40 μg/mL - •DPPH inhibition: <80 % [IV injection] - Dose: n.r. Injected daily (for 8 days)	+ Removing free radicals, exerting antioxidant effects + Promoting MN programming into anti-inflammatory M2 macrophages + Protecting and restoring cardiac function	[85]
Thrombosis (TB)	HMPB-rtPA@PM	SOD, CAT, POD-like activity	Inhibition of platelet aggregation and inflammation regulation	[In vitro] Conc. 500 μg/mL - H_2O_2 inhibition: <85 % - $O_2^{\bullet-}$ inhibition: <80 % - •OH inhibition: <80 % Conc. 100 μg/mL - O_2 generation: 45 mg/L (30 % H_2O_2 decompose) [IP injection] - Dose: 20 mg/kg, Injected for 24 h after starving at 20 °C for 8 h (6 days)	+ Scavenging ROS to break ROS-mediated oxidative stress cycle + Regulating local vascular inflammatory microenvironment + Inhibiting platelet aggregation	[92]
	PB-PFP@ PC	SOD, CAT, POD-like activity	Thrombus collapsion	[In vitro] Conc. 500 μg/mL - H_2O_2 inhibition: <68 % - $O_2^{\bullet-}$ inhibition: <80 % - •OH inhibition: <90 % Conc. 100 μg/mL - O_2 generation: 21 mg/L (30 % H_2O_2 decompose) [IV injection] - Dose: 4 mg/kg, Injection after laser therapy (7 days)	+ Regulating vascular microenvironment *via* its antioxidant activity + Providing antithrombosis to maximize antioxidant reaction + Reducing inflammatory factors in thrombus site	[93]

*ID: intradermally injection, IP: intraperitoneal injection.

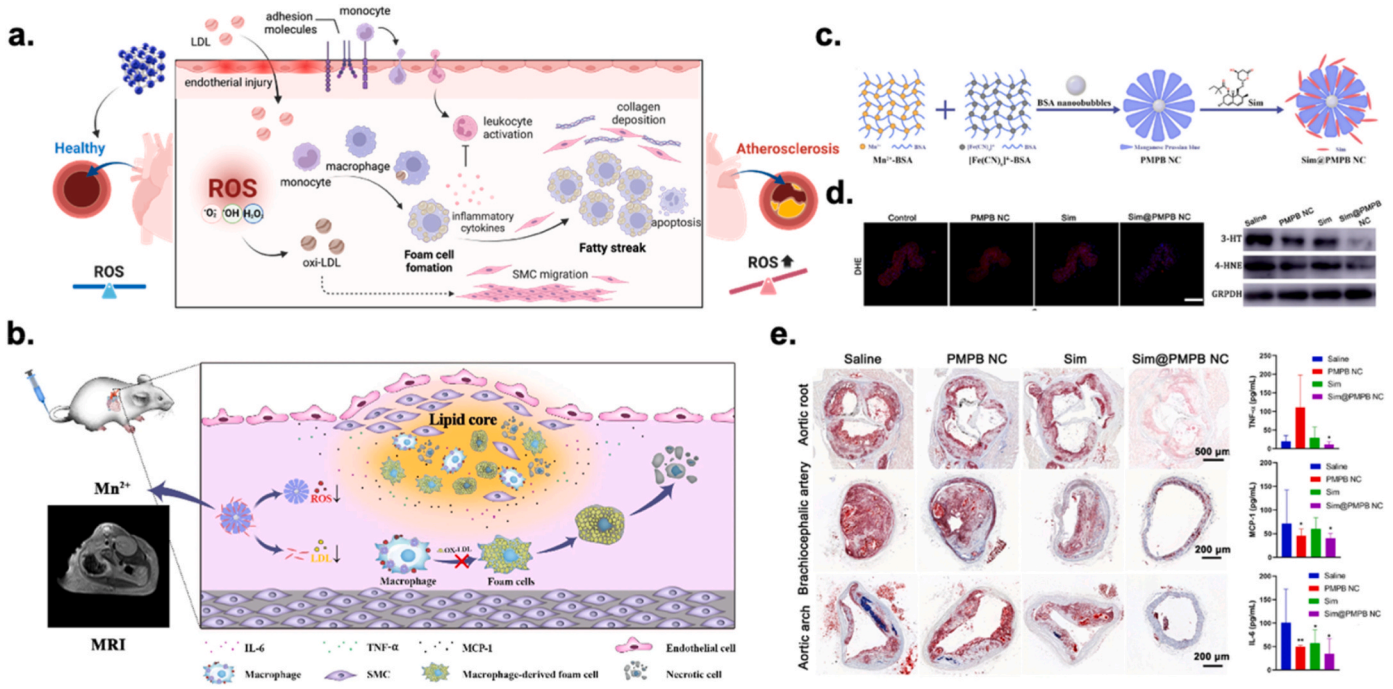

Fig. 9. (a) Role of ROS in atherosclerosis pathology and progression. (b) Schematic of underlying principle of using Sim@PMPB NC to treat atherosclerosis. (c) Schematic of synthesis of PMPB NC and Sim@PMPB NC. (d) Fluorescence images of DHE-stained sections of brachiocephalic artery after different treatments. (e) Theranostic effects of i.v.-delivered PMPB NC in ApoE$^{-/-}$ mice [86], Copyright 2021, Springer Nature.

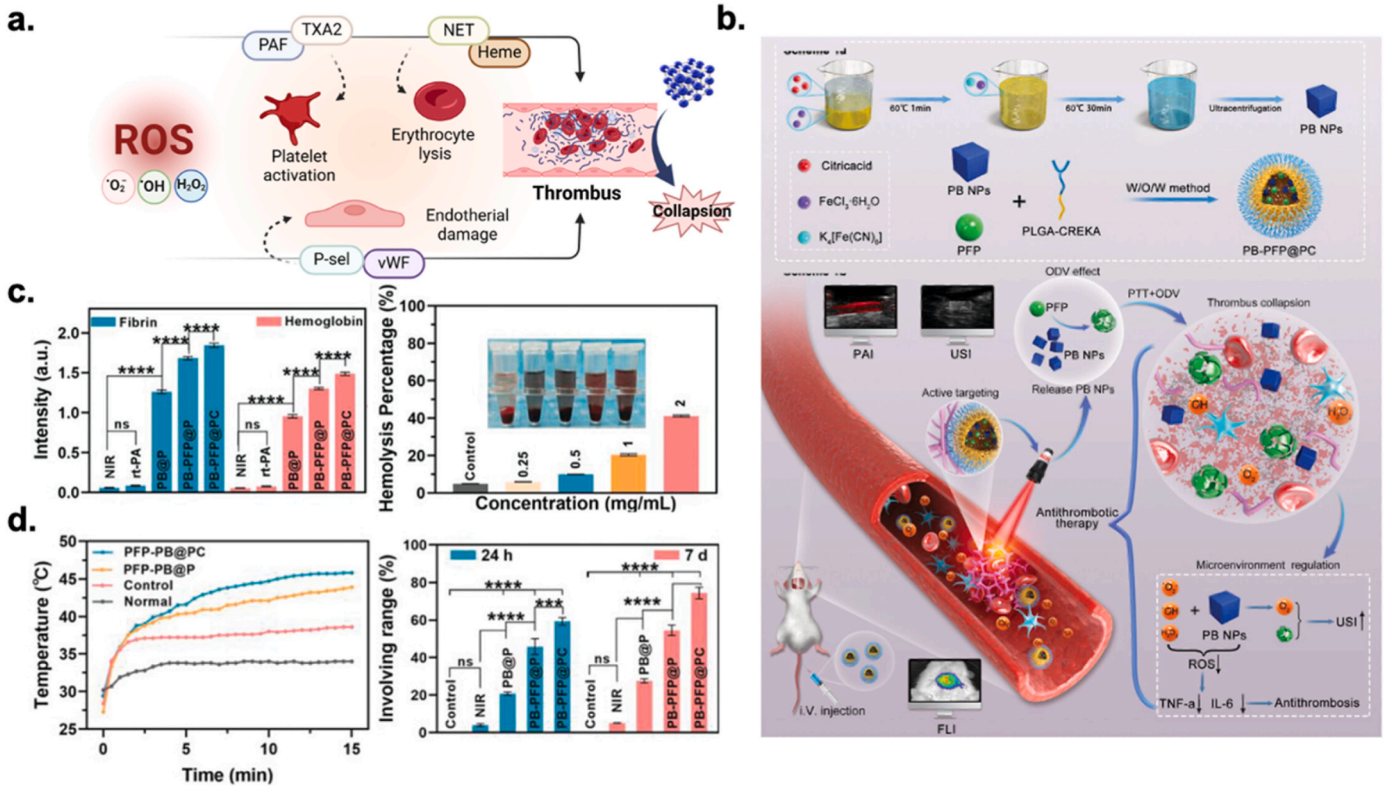

Fig. 10. (a) Role of ROS in thrombosis pathology and progression. (b) Schematic of PB-PFP@PC nanodroplet synthesis and PB-PFP@PC-mediated specific antithrombotic therapy. (c) Cell-based experiments and thrombolysis therapy *in vitro*. (d) Thrombolysis in antithrombotic therapy *in vivo*. Reprinted with permission [93], Copyright 2022, Wiley.

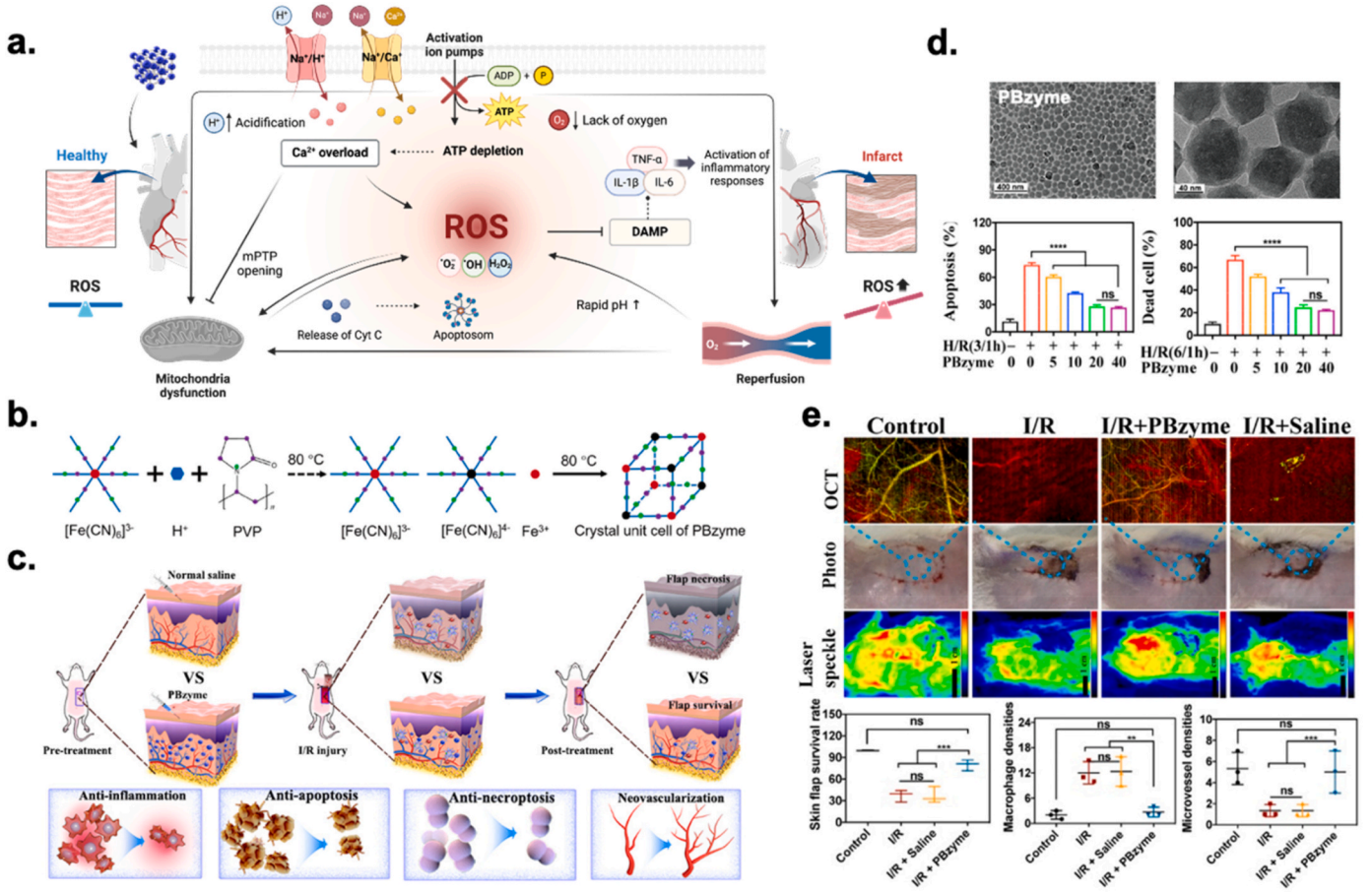

Fig. 11. (a) Role of ROS in ischemia reperfusion injury pathology and progression. (b) Schematic of PBzyme synthesis (c) Schematic of mechanism underlying PBzyme-mediated promotion of skin flap survival rate (d) TEM image and protective effect of PBzyme on hypoxia/reoxygenation-damaged *in vitro* model. (e) *In vivo* protective efficacy of PBzyme on I/R injured skin flap [76]. Copyright 2022, American Chemical Society.

significantly expedited wound size reduction in a diabetic murine model. Tang et al. fabricated KBP particles *via* PB amalgamation with konjac glucomannan and BSA [106]. In the subsequent phase, a KBP@KH hydrogel was developed using hydroxypropyl trimethyl ammonium chloride chitosan (HACC), which possesses inherent antibacterial properties. The KBP@KH hydrogel was administered to wounds inflicted in a type 2 diabetic rat model. The KBP@KH-treated group showed expedited wound healing and complete wound closure approximately 3–4 days earlier than in the control group. Furthermore, this intervention considerably augmented angiogenesis, as evidenced by a 33.12 % elevation in the development of novel blood vessels compared with that of the control cohort. Additionally, the KBP@KH hydrogel showed notable anti-inflammatory characteristics, as evidenced by the pronounced reduction in the expression levels of inflammatory mediators such as IL-6 and TNF-α. Tong et al. engineered CPB-Ce6 NPs for the comprehensive enhancement of wound healing by concurrently mitigating inflammatory responses and providing antibacterial activity [91]. They conceptualized a dual-functional agent that delivers oxygen to hypoxic environments at wound sites while effectively eradicating MRSA through photodynamic therapy (PDT) using the photosensitizer Ce6. In fact, the CPB-Ce6@G + L-treated cohort showed an approximate 98 % reduction in bacterial load in the wound area and significantly diminished presence of inflammatory cells, which advanced wound healing.

5.3.2. *Inflammatory bowel disease (IBD)*

IBD constitutes a persistent inflammatory disease that presents within the gastrointestinal system and is principally classified into ulcerative colitis (UC) and Crohn's disease (CD) [135]. ROS overproduction augments the intestinal mucosal barrier permeability, which facilitates pathogenic and bacterial invasion into the intestinal lumen, triggering inflammatory processes. Moreover, ROS overproduction disturbs the equilibrium of the intestinal microbiota and disrupts the antioxidant system, which consequently elevates the oxidative stress within the intestinal environment. This adversely impacts the functioning and survival of intestinal cells and hinders the regeneration and repair of the intestinal mucosa (Fig. 13a). In this context, ROS scavenging may improve the intestinal microenvironment by alleviating intestinal inflammation *via* PB.

Zhao et al. synthesized manganese PB nanozyme (MPBZ) and validated its therapeutic efficacy in the treatment of IBD based on ROS scavenging mechanisms and attenuation of inflammation [89]. MPBZ was designed based on its capacity to concentrate within the inflamed colonic mucosa owing to its particle size and surface charge, which act as targeting motifs. In a DSS-induced colitis mouse model, MPBZs improved weight loss, reduced colon length shortening, and decreased histological damage. Furthermore, MPBZs reduced the activity of myeloperoxidase, which is a well-established inflammatory biomarker, and those of pro-inflammatory cytokines such as IL-1β, IL-6, and TNF-α. This therapeutic action predominantly inhibited inflammation *via* the toll-like receptor (TLR) signaling pathway. Zhu et al. engineered a selenium-loaded manganese PB nanozyme (Se-HMPB) to confer an enhanced glutathione peroxidase (GPx) effect (Fig. 13b–d) [116]. The Se-HMPB showed notable efficacy in scavenging ROS, mitigating inflammation, inhibiting ferroptosis and T-cell differentiation owing to its GPx activity. The attenuation of T-cell differentiation effectively

Table 5
Therapeutic effect of PB in inflammatory diseases.

Diseases	Prussian Blue forms	Type of ROS scavenging	Target scavenging route	ROS scavenging efficacy/ Administration	Therapeutic effects	Ref
Wound Healing (WH)	KBP@KH hydrogel	SOD, CAT, POD-like activity	Inhibition chronic inflammation, promotion angiogenesis	[In vitro] Conc. n.r. - H_2O_2 inhibition: <75 % - •OH inhibition <80 % - $O_2^{\bullet-}$ inhibition: <70 % Conc. 100 μg/mL - DCFH-DA <70 % (L929 cells, ROS induced by 500 μg/mL H_2O_2) [Dermal wound healing] - Dose: n.r. (1 cm wound) Replaced every 2 days (for 14 days)	+ Absorbing tissue fluid outflow from wound site + Bactericidal and antibacterial effects + Protecting skin cells against ROS induced damage + Promoting cells growth + Anti-inflammatory and pro-angiogenic effects on wound healing processes	[106]
	CPB–Ce6 NPs	CAT, POD-like activity	Anti-bacterial, alleviation hypoxia	[In vitro] Conc. n.r. - O_2 generation: 21 mg/L [Dermal wound healing] - Dose: n.r. (MRSA-infected wound) (for 11 days)	+ Superior nanozyme activity and O_2 production capacity for antibacterial effects + Bacterial killing effect by PDT application in infected diabetic wound + Promoting diabetic wound healing *via* ROS scavenging	[91]
	PBNPs @PLEL	SOD, CAT, POD-like activity	Enhancement of mitochondrial function	[In vitro] Conc. 200 μg/mL - H_2O_2 inhibition: <90 % - $O_2^{\bullet-}$ inhibition: <40 % - •OH inhibition: <80 % Conc. 100 μg/mL - DCFH-DA <50 % ROS induced by H_2O_2 (HaCaTs 700 μM, HUVECs 600 μM, and HFs 300 μM) [Dermal wound healing] - Dose: n.r. (1 cm wound) Replaced every 4 days (for 14 days)	+ Protecting skin cells against oxidative stress-induced cell death + Restoring NRF2/HO-1 pathway activity + Restoring mitochondrial membrane potential and ATP production + Reducing calcium concentration in mitochondria + Promoting cutaneous diabetic wound healing by ROS scavenging and anti-inflammatory and pro-angiogenic activities	[110]
	PB@Lipo	CAT-like activity	Promotion M2 macrophage polarization	[In vitro] Conc. n.r. - CAT-activity: <28.5 % - GPx activity: <65 % [Dermal wound healing] - Dose: n.r. (for 14 days)	+ Excellent anti-inflammatory and antioxidant effects + Providing highest wound healing rate, collagen deposition, and tissue maturation + Promoting macrophage transformation from anti-inflammatory M1 to pro-inflammatory M2 phenotype	[105]
Inflammatory bowel disease (IBD)	Se-HMPB	SOD, CAT, POD-like activity	Inhibition of ferroptosis, regulation of T-cell differentiation	[In vitro] Conc. 100 μg/mL - GPx activity: <72 % - $O_2^{\bullet-}$ inhibition: <70 % - •OH inhibition: <65 % - O_2 generation: 18 mg/L - DCFH-DA <50 % (ROS induced by 3 mM H_2O_2 in NCM460 cells) [IV injection] - Dose: 10 mg/kg Injected every 3 days (for 15 days)	+ Protecting integrity of cell membrane of intestinal epithelial cells + Reconstructing intestinal mechanical barrier by inhibiting ferroptosis + Scavenging large number of ROS in inflammatory macrophages + Decreasing inflammatory factor levels	[116]
	MPBZs	SOD, CAT, POD-like activity	Inhibition of anti-inflammatory cytokines	[In vitro] Conc. 20 mg/L - •OH inhibition: <93 % - •OOH inhibition: <83 % Conc. 10 mg/L - H_2O_2 inhibition: <83 % [Oral administration] - Dose: 0.3 mg/mL, 0.3 mL Orally treated every 2 days (for 7 days)	+ Scavenging various ROS + Improving colitis by eliciting primary effect on TLR signaling pathway without adverse side effects	[89]
Bone-related Disease (BD)	PB @MSCM	SOD, CAT-like activity	Suppression of oxidative stress, decreased apoptosis-related gene expression	[*In vitro*] Conc. 40 μg/mL - SOD mimic activity: 40 U/mg - O_2 generation: 40 mg/L Conc. 55.5 μg/mL - H_2O_2 inhibition: <25 % [IV injection] - Dose: 15 mg/kg Injected within 2 h after IR	+ Scavenging overproduced ROS in irradiated-bone marrow cells + Mitigating hematopoietic cell apoptosis + Accelerating regeneration of hematopoietic stem and progenitor cells	[107]

(*continued on next page*)

Table 5 (*continued*)

Diseases	Prussian Blue forms	Type of ROS scavenging	Target scavenging route	ROS scavenging efficacy/ Administration	Therapeutic effects	Ref
	HPBZs	SOD, CAT, POD-like activity	Inhibition osteoclast formation and osteoclast resorption activity	[In vitro] Conc. 20 ppm Redox potential, - •OH/H_2O: 2.8 V - $O_2^{\bullet-}$/H_2O_2: 1.5 V - H_2O_2/H_2O: 1.776 V - DCFH-DA <90 % (ROS induced by 100 ng/mL RANKL in BMMs cells) [IV injection] - Dose: 0.72 mg/mL, 50 μL Injected twice a week (for 6 weeks)	+ Therapeutic effect against osteoporotic bone loss by normalizing OP microenvironment + Inhibiting osteoclast-genesis and bone resorption + Suppression of the mitogen-activated protein kinase, and nuclear factor kB signaling pathways + Regulating osteoclast differentiation and OP progression	[103]
	USPBNPs	SOD, CAT, POD-like activity	Promotion of M2 macrophage polarization, inhibition of proinflammatory cytokines	[In vitro] Conc. 10 μg/mL - $O_2^{\bullet-}$ inhibition: <86 % - •OH inhibition: <77 % Conc. 0.3 μg/mL - O_2 generation: 18 mg/L (0.3 M H_2O_2 decompose) Conc. 5 μg/mL - DCFH-DA <40 % (ROS induced by 1 mM H_2O_2 in primary synovial cells) [Local injection] - Dose: 0.5 mg/mL, 50 μL Injected into joint cavity of OA rats every week (for 4 weeks)	+ Decreasing secretion of proinflammatory cytokines + Inducing transition of proinflammatory M1 macrophages to anti-inflammatory M2 macrophages by ROS scavenging + Regulating ROS and oxygen levels in cellular microenvironment + Therapeutic effect against osteoarthritis	[81]

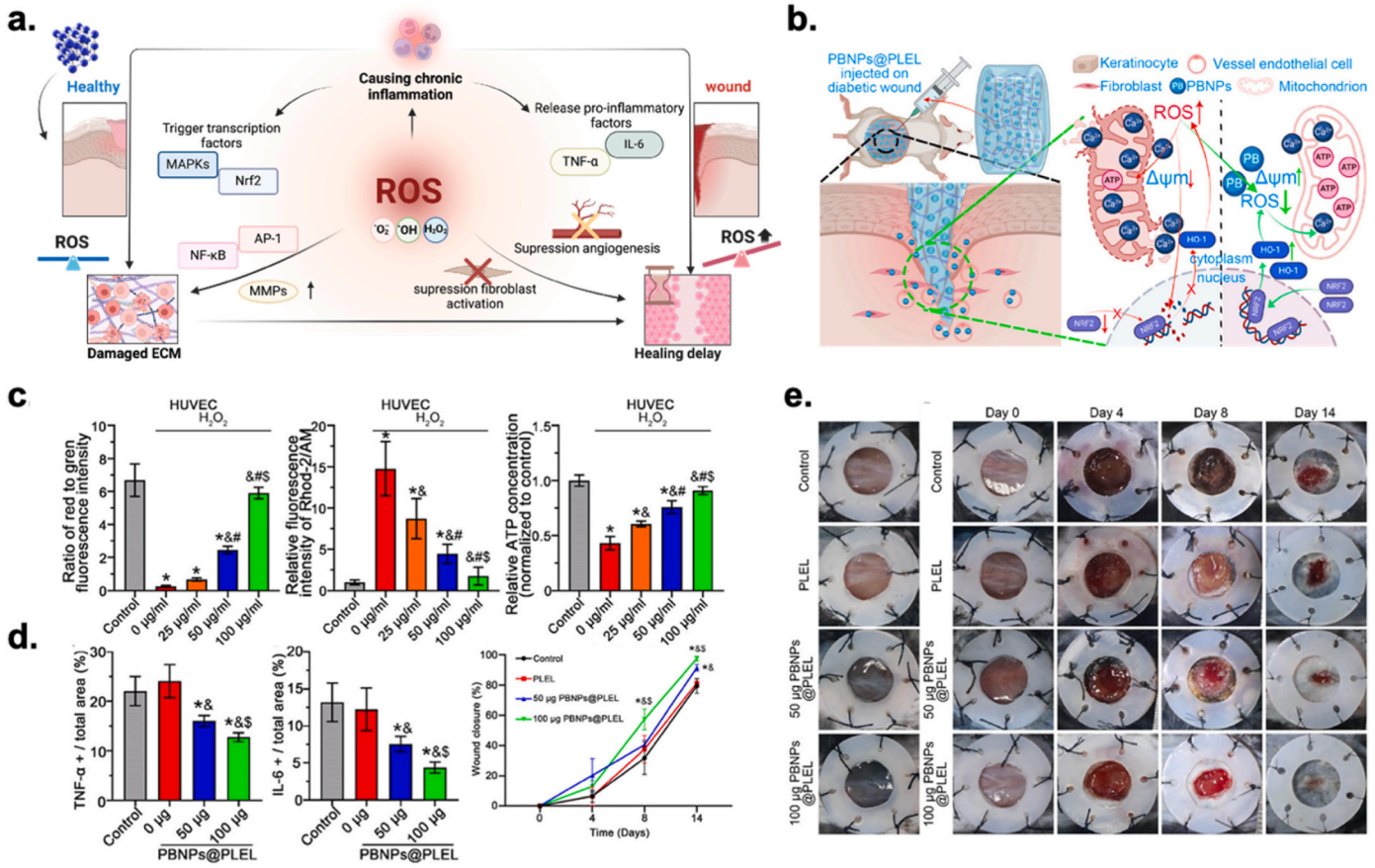

Fig. 12. (a) Role of ROS in wound pathology and progression. (b) Schematic of use of PBNPs@PLEL for enhancement of diabetic wound healing. (c) Effect of PBNPs@PLEL in restoring mitochondrial function. (d) Pro-inflammatory cytokine inhibitory effect of PBNPs@PLEL. (e) Experimental images of *in vivo* wound healing [110]. Copyright 2022, American Chemical Society.

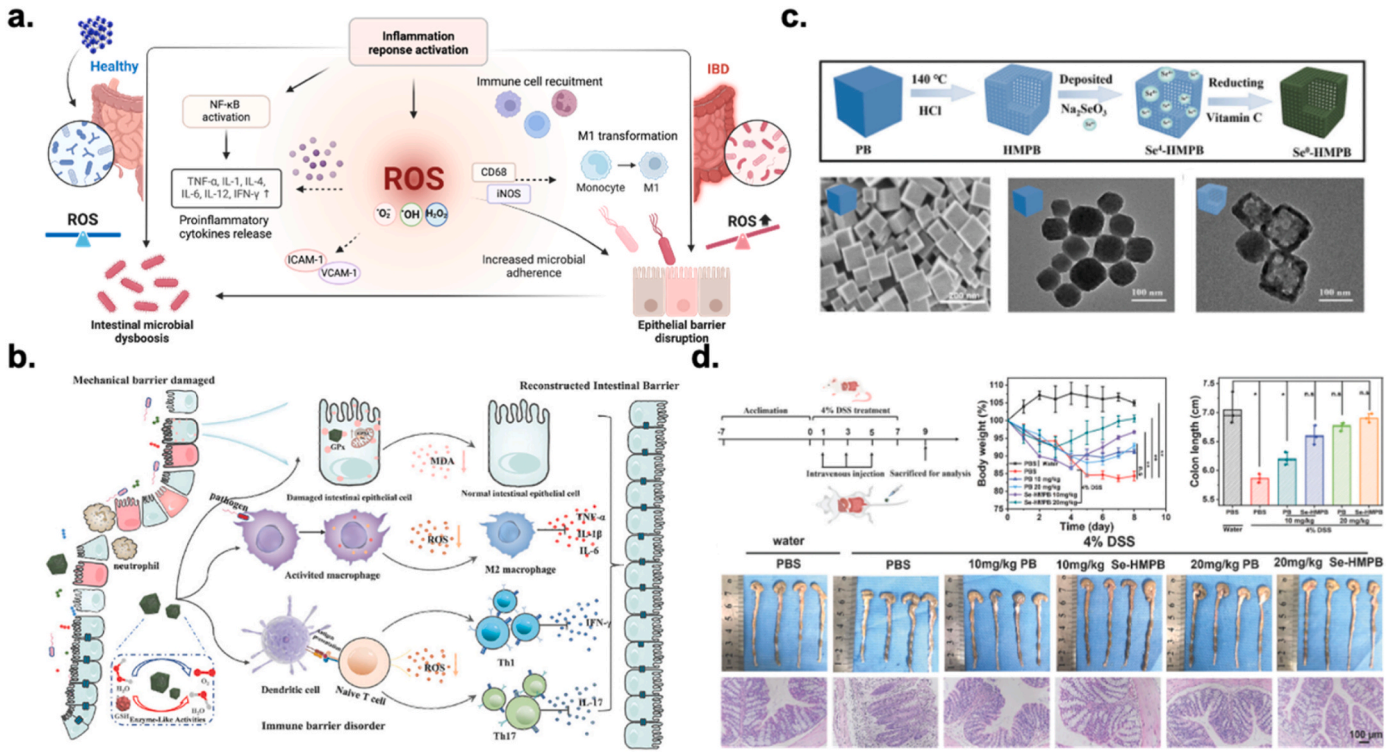

Fig. 13. (a) Role of ROS in inflammatory bowel disease pathology and progression. (b) Schematic of effect of Se-HMPB nanozyme in reconstructing intestinal barrier against inflammatory bowel disease. (c) Synthesis and TEM images of Se-HMPB. (d) Preventive effects of PB and Se-HMPB nanozyme in DSS-induced colitis mice model. Reprinted with permission [116], Copyright 2023, Wiley.

modulated excessive immune responses and preserved intestinal immune barrier integrity. Moreover, Se-HMPB successfully prevented weight loss, enhanced colon length, and alleviated damage to the intestinal mucosa in UC and DC models.

5.3.3. *Bone-related disease (BD)*

Arthritis is a chronic inflammatory bone-related disease (BD) that is accompanied by pain, swelling, and joint stiffness [136]. Arthritis is primarily categories into age-related osteoarthritis and rheumatoid arthritis, which is also classified as an autoimmune disorder. Excessive ROS degrade collagen and proteoglycan (PG), which are the primary components of the bone matrix. This induces the apoptosis of chondrocytes, which reduces the regenerative ability of the cartilage by retaining a chronic inflammatory state. ROS accumulation further activates osteoclast formation and inhibits osteoblast activation, which results in bone loss (Fig. 14a) [137]. Therefore, PB-based antioxidant therapy may effectively attenuate bone loss and improve bone microstructure by reducing ROS levels and inflammatory responses in arthritis.

Ye et al. suggested a template-free porous PBzyme (HPBZ) using Bi^{3+}. Furthermore, they examined its therapeutic implications in the context of osteoporosis (Fig. 14b–d) [103]. The HPBZs diminished ROS levels, which obstructed NF-κB activation and MAPK signaling cascades. The diminished expression of osteoclast-associated transcription factors decreased both the quantity and dimension of osteoclasts. In an ovariectomized murine model, osteoclast activity was inhibited, which reduced bone resorption and enhanced bone microarchitecture. Thus, osteoporosis progression was delayed. Qin et al. elucidated the therapeutic efficacy of ultrasmall PBNPs in treating osteoarthritis. They successfully prepared ultrasmall USPBNPs that were approximately 3.5 nm in size and used a specific ethanol (75 % EtOH) concentration to improve the biological efficacy [81]. The USPBNPs downregulated ROS levels and helped polarize the macrophages from the M1 to M2 phenotype, which lowered the expression of pro-inflammatory cytokines such as IL-6, TNF-α, and MMP-13. Through this anti-inflammatory mechanism, USPBNPs alleviated joint edema in an animal model of osteoarthritis and mitigated chondrocyte injury, leading to a sustained effect of decelerating osteoarthritis progression. Zhang et al. showed the effectiveness of mesenchymal stem cell membrane (MSCM)-coated PB in alleviating radiation-induced damage in the bone marrow and enhancing hematopoietic regeneration [107]. The MSCM coating was used to improve the targeting efficacy at the compromised bone marrow. The PB@MSCM elicited protective effects on mitochondria and anti-apoptotic properties *via* ROS scavenging. Reduction in the apoptosis of the hemopoietic stem/progenitor cells (HSPCs) promoted hematopoietic regeneration. Thus, the PB@MSCM-treated group showed confirmed recovery of bone marrow cells, as was clearly evidenced by the increase in the total number of bone marrow-derived colony-forming units (CFUs).

5.4. *Other diseases*

ROS incite considerable damage throughout the entire organism (Fig. 15a, Table 6). In the spinal region, ROS expedite intervertebral disc (IVD) degeneration and induce inflammation in the adjacent musculature and ligaments, which results in persistent pain [138]. The nucleus pulposus cells (NPCs) that reside in the IVD are typically situated in a hypoxic environment; however, ROS-mediated disc damage induces a transition to a slightly hyperoxic state, which triggers inflammatory responses, cellular apoptosis, and proliferation. Consequently, ROS elimination through PB application may potentially ameliorate IVD degeneration by salvaging the NPCs. Zhou et al. introduced a potential biotherapeutic PB agent to attenuate IVD degeneration and minimize oxidative stress in the NPCs [77]. PBNPs diminished intracellular oxidative stress through several underlying mechanisms such as enhancing mitochondrial functionality, stabilizing SOD1, and facilitating ECM synthesis. Through these mechanisms, PBNPs effectively impeded disc degeneration in a rat caudal puncture model, as evidenced

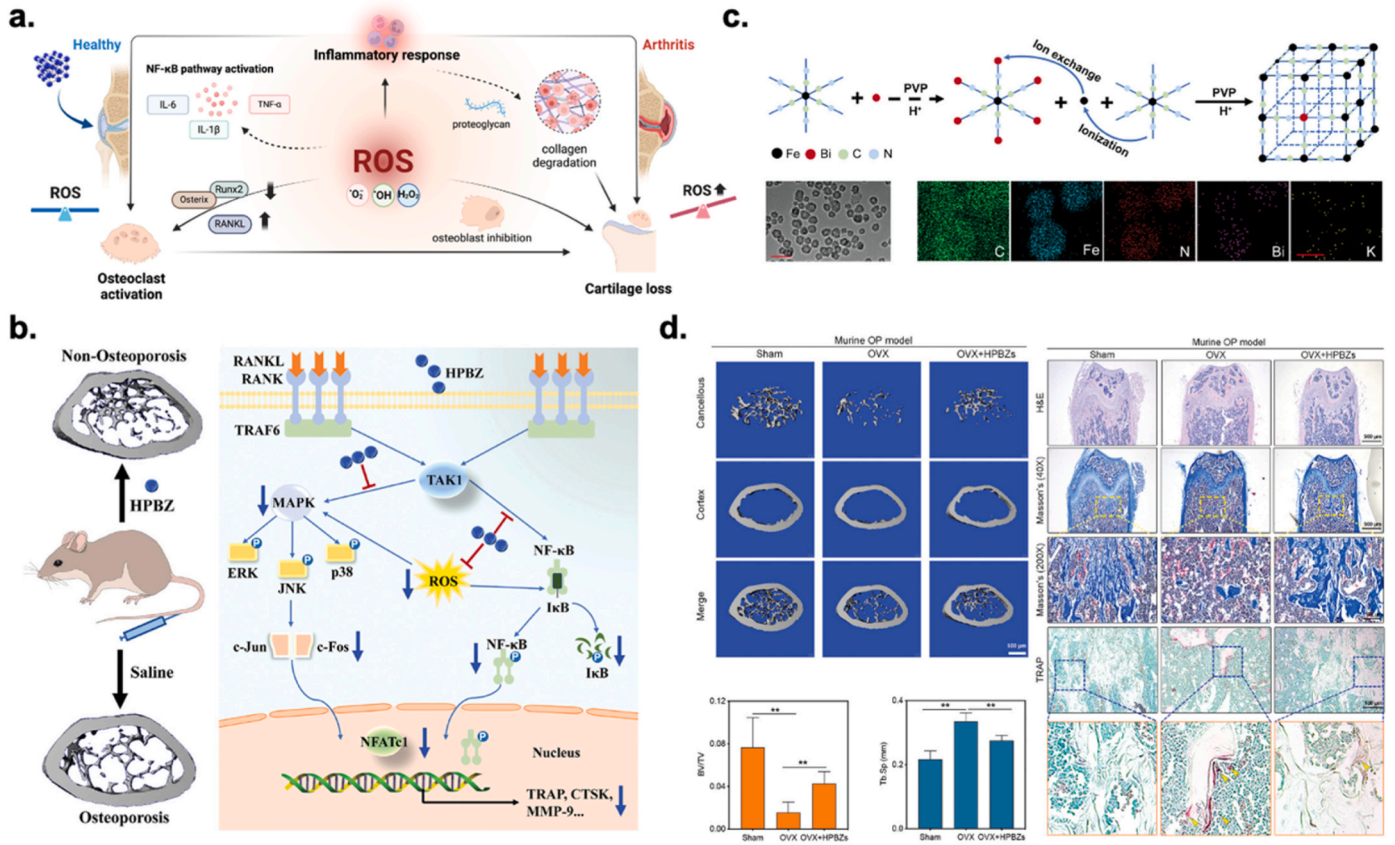

Fig. 14. (a) Role of ROS in osteoarthritis pathology. (b) Schematic of HPBZ-mediated normalization of disease microenvironment for treatment of osteoporosis (OP). (c) Synthesis and TEM images of HPBZ. (d) Representative 3D micro-CT images of distal femur specimens, and quantification of bone-to-tissue volume ratio and trabecular separation. Reprinted with permission [103]. Copyright 2022, Wiley.

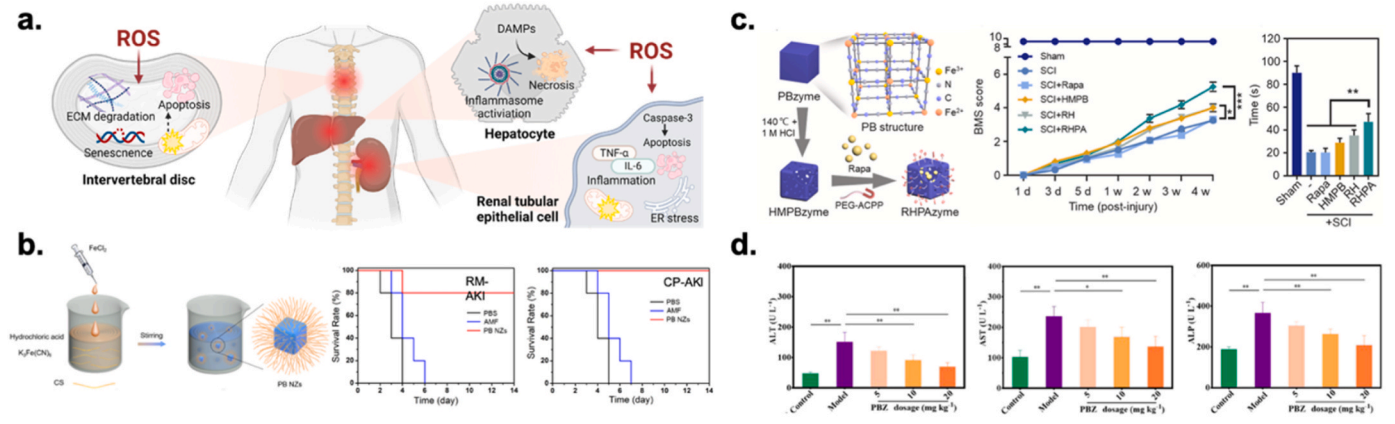

Fig. 15. (a) Role of ROS in various organ failures. (b) Schematic of PBNZs synthesis and survival rate in RM-AKI and CP-AKI [95]. Copyright 2021, Springer Nature. (c) Schematic of PBzyme synthesis; assessment of motor function in hindlimbs based on BMS score and total run time of mice using totarod test. Reprinted with permission [94], Copyright 2023, Elsevier Ltd. (d) ALT, AST, and ALP levels in the serum from AILI mouse [78]. Copyright 2021, American Chemical Society.

by the restoration of disc height and structural integrity.

AKI is a pathological state characterized by rapid decline in renal function because of disrupted blood flow, renal damage, and inflammation [139]. ROS are intricately associated with AKI because they facilitate vascular dysfunction, inflammatory responses, and cytotoxicity in renal tubules. Thus, antioxidant treatment may yield beneficial effects in mitigating the deleterious consequences associated with AKI. Zhang et al. have developed ultrasmall PB nanoparticles (PBNZs) comprising chitosan (CS) as templates for a theragnostic approach for curing AKI (Fig. 15b) [95]. The PBNZs protected renal cells against oxidative stress and exhibited enhanced therapeutic efficacy similar to that of the conventional pharmacological agent amifostine in two distinct AKI models, which were induced either using rhabdomyolysis or cisplatin administration. This improved efficacy may be attributed to the reduced expression levels of KIM-1 and HO-1, which are the principal biomarkers of renal injury, and normalized SOD levels observed in the PBNZ treatment cohort.

A subsequent study investigated and confirmed the therapeutic efficacy of PB in the intricate framework of SCI characterized by concomitant ischemia and hypoxia. SCI is a critical clinical condition

Table 6
Therapeutic effect of PB in other diseases.

Diseases	Prussian Blue forms	Type of ROS scavenging	Targeting scavenging route	ROS scavenging efficacy/ Administration	Therapeutic effects	Ref
Intervertebral Disc (IVD)	PBNPs	SOD, CAT, POD-like activity	Enhancement of mitochondrial function, stabilization of SOD1, promotion of ECM synthesis	[*In vitro*] Conc. 50 μg/mL - $O_2^{\bullet-}$ inhibition: <80 % - •OH inhibition: <90 % (1 mM H_2O_2 decompose) - GPx activity: <60 % Conc. 500 ng/mL - H_2O_2 inhibition: <22.8 % Conc. 2 μg/mL - DCFH-DA <41 % (ROS induced by 0.0006 % H_2O_2 in NPCs) [Local injection] - Dose: 2 μg, 0.2 μg (5 μL) (for 4 weeks)	+ Alleviating intracellular oxidative stress + Increasing intracellular activities of superoxide dismutase 1 (SOD1) + Rescuing nucleus pulposus cell degeneration + Improving mitochondrial structure to increase antioxidation ability + Rescuing ROS-induced IVD	[77]
Organ Failure (OF)	PB NZs	SOD, CAT, POD-like activity	Reduced apoptosis, normalization of SOD levels	[*In vitro*] Conc. 100 μg/mL - $O_2^{\bullet-}$ inhibition: <75 % - •OH inhibition: <80 % Conc. 50–200 μg/mL - •ABTS inhibition: <89 % - •DPPH inhibition: <23 % - O_2 generation: 12 mg/L (3 % H_2O_2 decompose) - DCFH-DA <70 % (ROS induced by 0.5 mM H_2O_2 in HEK293T cells) [IP injection] - Dose: 100 μg/100 μL Injected 2-h after cis-platinum treatment (for 14 days)	+ Protecting cellular environment from H_2O_2- induced damage + Promoting effective elimination of RONS + Reducing BUN and CRE levels + Effective restoration of kidney function	[95]
	PBZs	SOD, CAT, POD-like activity	Inhibition of hepatocyte apoptosis; reduction of inflammatory cytokines levels and infiltration of neutrophils and macrophages	[In vitro] Conc. 100 μg/mL - POD-like activity: <94 % - $O_2^{\bullet-}$ inhibition: <55 % - •OH inhibition: <60 % - O_2 generation: 18 mg/L Conc. 25 μg/mL POD activity < Conc. 100 μg/mL - DCFH-DA <50 % (ROS induced by 5 μM DNR in AML12 cells) [IV injection] - Dose: 20 mg/kg Injected 2-h before DNR treatment (for 24 h)	+ Protecting AML12 cells from oxidative stress-induced apoptosis + Preventing AILI by accumulating in the liver + Reducing overproduced ROS levels and inflammation + Reducing hepatocyte apoptosis + Increasing antioxidant enzyme levels + Suppressing inflammatory cytokine levels + Upregulating antioxidative genes by activating the Nrf2/ARE pathway + Aiding neutrophil and macrophage infiltration	[78]
	RHPAzyme	SOD, CAT, POD-like activity	Mitigating mitochondrial dysfunction, Inhibition of apoptosis, promotion of M2 macrophage polarization	[*In vitro*] Conc. 45 μg/mL - •ABTS inhibition: <25 % Conc. 40 μg/mL - $O_2^{\bullet-}$ inhibition: <94 % - •OH inhibition: <30 % - GPx activity <25 % - SOD activity <95 % - CAT activity <25 % Conc. 1 μg/mL - DCFH-DA <50 % (ROS induced by 0.1 μg/mL Rapa in SH-SY5Y) [IV injection] - Dose: 10 mg/kg Injected daily (for 5 days)	+ Scavenging overproduced ROS + Reducing inflammation in oxygen–glucose deprivation (OGD)-induced damage signaling pathway + Promoting motor function recovery + Inhibiting oxygen-mediated cell apoptosis + Suppressing inflammation-induced injury + Reducing nervous impairment	[94]

that results from spinal cord damage [140]. ROS exacerbate neuro-inflammation and cellular apoptosis in the spinal cord, which exacerbate tissue injury [141]. However, PB-derived antioxidant therapeutic agents mitigated inflammation and attenuated SCI-associated damage. Shen et al. developed newly formulated RHPAzyme by incorporating rapamycin [94]. RHPAzyme acts as an immunosuppressive agent in PBNPs to achieve synergistic therapeutic effects. Additionally, it modifies the surface with activated cell-penetrating peptides to enhance stability and facilitate targeted delivery to the injury site (Fig. 15c). An *in vitro* study in an oxygen-glucose deprivation (OGD) neuroblastoma cell model confirmed the efficacy of RHPAzyme in alleviating mitochondrial dysfunction, diminishing ROS levels, and inhibiting apoptosis. Furthermore, RHPAzyme promoted the polarization transition from M1 to M2 macrophages, which reduced inflammatory responses. In an SCI mouse model, RHPAzyme exerted a neuroprotective effect by activating the PI3K/AKT/mTOR signaling cascade, which promoted motor function recovery.

Liver failure (LF, hepatic impairment) is a significant side effect of anticancer drugs such as daunorubicin (DNR) and doxorubicin (DOX) and potentially leads to serious complications [142]. DNR-induced toxicity is intricately linked to ROS overproduction because it leads to lipid peroxidation and cellular injury, which exacerbate inflammatory responses. Therefore, ROS scavenging is a viable strategy for protection against hepatic injury. Bai et al. studied the prevention of anthracycline-induced liver injury (AILI) using PVP-modified PB particles (Fig. 15d) [78]. PBZ exhibited therapeutic efficacy by attenuating ROS-mediated hepatocyte apoptosis, diminishing DNA damage, and lowering the concentrations of inflammatory cytokines. Additionally, in an AILI mouse model, PBZ enhanced hepatic function by inhibiting HMGB-1 expression and augmenting antioxidant activity *via* the activation of the Nrf2 signaling pathway.

6. Stability and biocompatibility of PB

The clinical application of nanoparticles has been long hindered by concerns of their stability [143,144]. Novel nanoparticle concepts have been constantly emerging, but obtaining regulatory approval as practical medical technologies remains a challenging and distant goal [145]. Extensive studies in the biomedical field have determined that the size, morphology, and electrostatic charge of the nano-sized materials significantly affect their biocompatibility and biological stability [146–148]. Consequently, numerous challenges need to be addressed to translate nanoscale therapeutics to clinical practice [149,150].

However, PB differs from other nanoparticles because it has already been approved by the US FDA as an oral therapeutic for acute and chronic thallium and cesium poisoning. The International Atomic Energy Agency (IAEA) has recommended a daily intake of approximately 6 g for adults with an upper limit of 10 g for adult males [74]. Previously reported side effects of PB include abdominal pain and constipation among patients and possible hypokalemia and nutritional imbalance among healthy individuals [151,152]. Thus, PB has an established safely baseline level and precise design. Therefore, it shows high potential as a therapeutic candidate with high biocompatibility and stability.

PB exhibits notable physicochemical properties such as variable size and morphology (cubic, circle, polyhedral) and capacity to modify its chemical composition by incorporating diverse metal ions. These advantages have recently garnered recognition for PB as a potential therapeutic agent in the biomedical field. However, the crucial fact to be acknowledged is that PB has been approved by the FDA only for oral administration, and several parameters such as size, surface area, shape, and electrostatic characters need to be carefully evaluated. In 2020, Wang et al. demonstrated the biosafety and biocompatibility of various PB forms that exhibited different sizes, morphologies, and surface electrostatic properties [15]. They used citric acid at different concentrations to synthesize PB particles at various sizes. They induced variation in charge using the positively charged polymer polyethyleneimine (PEI). Additionally, they synthesized spherical and cubic PB nanoparticles using validated protocols. Then, they performed evaluation and found that most formulations showed high stability in aqueous and serum-containing media for up to 5 days with the only exception being the positively charged PB. Furthermore, PB retained its enzymatic activity as a nanozyme, and the hemolysis rates remained below the ISO standard of 5 %. This indicates excellent biocompatibility. *In vivo* toxicity evaluations showed transient elevations in liver and kidney function markers at 6–12 h after PB administration, after which they returned to normal levels. Furthermore, no residual PB was observed in major organs after approximately 2 weeks of repeated dosing. This confirms its efficient clearance through metabolic processes.

Similar studies have evaluated PB stability under various conditions such as polymer coatings or magnetic properties; furthermore, its compatibility with normal and cancer cells have been assessed [153,154]. Fu et al. found that PB displayed minimal long-term toxicity in the absence of photothermal irradiation [155]. Multiple studies have confirmed that irrespective of the synthesis technique used to fabricate different PB forms, it exhibited notably high biological stability at the tissue level in animal models [156]. This indicates the high potential of PB to adapt to diverse technological combinations.

We have summarized the biostability and biocompatibility evaluation results of PB-based therapeutics for ROS scavenging-mediated therapy in Table 7. This review aims to provide comprehensive insights for researchers in the biomedical field to enable the rational designing and engineering of ROS-related biotherapeutics to accelerate their progression to clinical stages.

7. Conclusion and perspective

This review has systematically summarized the biological application of PB-based materials in ROS-associated disease therapy. We have elucidated the pathological role of ROS for each disease category and used this as a basis for comprehensively exploring the therapeutic effect of the ROS-scavenging activity exhibited by PB-based materials. Additionally, the excellent enzyme-mimicking properties result in superior ROS scavenging efficacy, further demonstrating the significant potential of PB-based materials for ROS-associated disease therapy. In addition to their catalytic efficacy, they show notably high biocompatibility, facile synthesis methods, and versatility in various engineering approaches, which are advantageous for the practical implementation of PB in medicine. Furthermore, the inherently high photothermal and physicochemical properties of PB enable its use in various biomedical areas such as cancer therapy, imaging, and diagnosis and as theragnostic agents with catalytic properties. However, the use of pristine PB has been limited by its non-specific disease targeting efficiency. To overcome this hurdle, various modification engineering approaches are applied to PB for imparting specific capabilities. For example, cell membrane coating enhances immune cell targeting ability and facilitates increased accumulation in lesion sites. Therefore, further studies are needed to establish methods to overcome the inherent limitations of PB by implementing modified engineering strategies that would enhance their potential as therapeutic agents. FDA approval for PB as a drug validates its safety profile; however, this approval applies to its pristine formulation and non-engineered form. Hence, systemic evaluation according to engineering parameters such as size, porosity, morphology, and type of modification should be performed for safety validation. Furthermore, most studies have reported the *in vivo* intrinsic particle stability, clearance profile, and degradation behavior, but long-term safety implications of residual PB are yet to be comprehensively elucidated. Implementing comprehensive improvements based on these considerations would accelerate the clinical translation and broaden the practical therapeutic applications of PB in disease treatment.

Overall, PB exhibits potential as a multi-therapeutic modality owing to its unique physicochemical properties. Its applications extend beyond drug-based formulations such as drug delivery patches for wound

Table 7
Stability and biocompatibility of PB-based therapeutics.

Type	Disease	Prussian Blue forms	Stability	Biocompatibility	Ref
Neurological Disease (ND)	AD	PBNPs	- Morphological: n.r - Functional: n.r.	- In-vitro: n.r.	[88]
		PB/RBC	- Morphological: at least 7 days stable (Intact morphology, size) - Functional: sustained superior catalytic function	- In-vitro: >90 % cell viable in H-SY5Y, bEnd.3, BV2 (Conc.: ~40 μg/mL)	[90]
		PBK NPs	- Morphological: at least 7 days stable in water, PBS, DMEM (Intact morphology, size) - Functional: sustained superior catalytic function - Thermal: sustained photothermal effects	- In-vitro: >90 % cell viable in PC12, SH-SY5Y (Conc.: ~200 μg/mL)	[104]
	PD	PBzyme	- Morphological: at least 7 days stable in saline (Intact morphology, size) - Functional: sustained superior catalytic function	- In-vitro: >90 % cell viable in BV2, SH-SY5Y (Conc.: ~80 μg/mL)	[80]
	Stroke	PBzyme	- Morphological: at least 90 days stable (Intact morphology, size) - Functional: sustained superior catalytic function	- In-vitro: >90 % cell viable in BV2 (Conc.: ~100 μg/mL)	[79]
		PB@PDA	- Morphological: n.r. - Functional: sustained superior catalytic function	- In-vitro: >90 % cell viable in mouse primary neuron, microglia, astrocytes (Conc.: ~80 μg/mL)	[83]
		MPBzyme@NCM	- Morphological: at least 28 days stable in saline, serum (Intact hydrodynamic size) - Functional: n.r.	- In-vitro: >90 % cell viable in BV2, bEnd.3, SH-SY5Y (Conc.: ~40 μg/mL)	[82]
Cardiovascular Disease (CVD)	AS	HA-M@PB@ (PC + ART)	- Morphological: n.r. - Functional: n.r.	- In-vitro: >90 % cell viable in RAW264.7, VSMCs, HUVECs (Conc.: ~100 μg/mL)	[84, 86]
		Sim@ PMPB NC	- Morphological: at least 24 h stable in PBS (Intact hydrodynamic size with high colloidal stability) - Functional: n.r.	- In-vitro> 90 % cell viable in RAW264.(Conc.: ~400 μg/mL) - In-vivoInsignificant toxicity in female Kunming mic(Conc.: ~20 mg/kg, 24 days)	[84, 86]
		n-PBEs	- Morphological: at least 7 days stable in PBS, water, DMEM, FBS, Saline (Intact hydrodynamic size with high colloidal stability) - Functional: n.r.	- In-vitro> 90 % cell viable in RAW264.7, HUVECs, MOVASs (Conc.: ~200 μg/mL) - In-vivo: Insignificant toxicity in female Kunming mice (Conc.: ~10 mg/kg, 30 days)	[75]
	TB	HMPB-rtPA@PM	- Morphological: at least 7 days stable (Intact morphology, size) - Functional: n.r.	- In-vitro: >90 % cell viable in HUVECs: (Conc.: ~500 μg/mL) - In-vivo: Insignificant toxicity in Kunming mice (14 days)	[92]
		PB-PFP@ PC	- Morphological: at least 7 days stable in 10 % FBS + PBS (Intact hydrodynamic size) - Functional: n.r.	- In-vitro: >90 % cell viable in RAW264.7, HUVECs (Conc.: ~4 mg/mL) - In-vivo: Insignificant toxicity in Kunming mice (Conc.: ~4 mg/mL 21 days)	[93]
	IRI	PBzyme	- Morphological: n.r. - Functional: n.r.	- In-vitro: >90 % cell viable in HUVECs: (Conc.: ~160 μg/mL)	[76]
		PB Scavengers	- Morphological: at least 7 days stable in PBS (Intact morphology, size) - Functional: n.r.	- In-vitro: >90 % cell viable in Primary hepatocytes (Conc.: ~100 μg/mL)	[115]
		DSS/PB @BSP	- Morphological: at least 2 days stable in PBS (10 % FBS), blood (Intact morphology, size) - Functional: n.r.	- In-vitro: >80 % cell viable in RAW264.7 (Conc.: ~10 μg/mL)	[85]
Inflammatory Disease (ID)	WH	PB@Lipo	- Morphological: at least 7 days stable at 4 °C (Intact hydrodynamic size) - Functional: n.r.	- In-vivo: Insignificant toxicity in C57BL/6 mice (Conc.: ~0.1 mg/mL, 14 days)	[105]
		KBP@KH hydrogel	- Morphological: n.r. - Functional: (KBP) stable ROS scavenging efficacy	- In-vitro: >90 % cell viable in L929 (Conc.: ~100 μg/mL) - In-vivo: Minimum toxicity	[106]
		CPB–Ce6 NPs	- Morphological: at least 7 days stable in aqueous solution (Intact hydrodynamic size) - Functional: n.r.	- In-vitro: >90 % cell viable in NIH-3T3 cells, erythrocytes, HUVECs (Conc.: ~20 μg/mL, ~25 μg/mL, ~15 μg/mL) - In-vivo: Insignificant toxicity in BALB/C mice (Conc.: n.r., 11 days)	[91]
		PBNPs @PLEL	- Morphological: n.r. - Functional: n.r. - Structural: sustained stable hydrogel form	- In-vitro: >90 % cell viable in HUVECs, HaCaT, HF (Conc.: ~200 μg/mL)	[110]
	IBD	Se-HMPB	- Morphological: at least 7 days stable (Intact hydrodynamic size) - Functional: n.r. - Thermal: at least 3 days stable at various temperatures (4 °C, 25 °C, 37 °C)	- In-vitro: >90 % cell viable in HUVECs, NCM460 (Conc.: ~300 μg/mL) - In-vivo: Insignificant toxicity in BALB/C mice (Conc.: 40 mg/kg, 30 days)	[116]
		MPBZs	- Morphological: at least 3 days stable in pH 1 (Intact hydrodynamic size) - Functional: n.r.	- In-vitro: >90 % cell viable in DLD-1 (Conc.: ~80 ppm) - In-vivo: Insignificant toxicity in BALB/C mice (Conc.: 18 mg/kg, 14 days)	[89]
	BD	PB@MSCM	- Morphological: at least 5 days stable in PBS, 10 % FBS + PBS, RT (Intact hydrodynamic size) - Functional: n.r.	- In-vitro: >90 % cell viable in BM Lin^-, MS-5 (Conc.: ~100 μg/mL) - In-vivo: Insignificant toxicity in C57BL/6 mice (Conc.: 15 mg/kg, 14 days)	[107]

(*continued on next page*)

Table 7 (*continued*)

Type	Disease	Prussian Blue forms	Stability	Biocompatibility	Ref
		HPBZs	- Morphological: n.r. - Functional: n.r.	- In-vitro: >90 % cell viable in BMMs (Conc.: ~36 μg/mL)	[103]
		USPBNPs	- Morphological: at least 7 days stable, RT (Intact hydrodynamic size) - Functional: n.r.	- In-vitro: >90 % cell viable in THP-1 (Conc.: ~10 μg/mL)	[81]
Other Disease (OD)	IVD	PBNPs	- Morphological: n.r. - Functional: n.r.	- In-vitro: >90 % cell viable in NPCs, 293T (Conc.: ~3.125 μg/mL)	[77]
	Spinal	RHPAzyme	- Morphological: at least 7 days stable in PBS, DMEM (+10 % FBS) - Functional: n.r.	- In-vitro: >90 % cell viable in SH-SY5Y (Conc.: ~10 μg/mL)	[94]
	kidney	PBNZs	- Morphological: at least 7 days stable in PBS, DMEM, FBS (Intact hydrodynamic size) - Functional: n.r.	- In-vitro: >90 % cell viable in HEK239T (Conc.: ~200 μg/mL) - In-vivo: Insignificant toxicity in BALB/C mice (Conc.: 50 mg/kg, 14 days)	[95]
	Liver	PBZs	- Morphological: at least 7 days stable in water, saline, DMEM at 4 °C, 25 °C, 37 °C (Intact hydrodynamic size) - Functional: n.r.	- In-vitro: >90 % cell viable in AML12 (Conc.: ~100 μg/mL) - In-vivo: Insignificant toxicity in BALB/C mice (Conc.: 25 mg/kg, 7 days)	[78]

healing and electrostimulation-combined systems because of its ability to integrate with various therapeutic systems. In terms of tissue engineering applications, it can be used in scaffolds, hydrogels, and coating materials for implant surface modification. These diverse applications as tissue engineering material significantly expand the potential of PB in regenerative medicine. Furthermore, these multidimensional application possibilities suggest that PB possesses extensive potential as an advanced medical material beyond simple therapeutics. Therefore, the development of various PB-based medical materials is expected to provide innovative therapeutic options in next-generation biomedicine applications.

8. Review methodology

This study highlights the crucial role of designing PB-based biotherapeutic materials in biomedical research for treating various ROS-related diseases. We conducted this review by extensively concentrating on PB synthesis strategies, underlying ROS generation mechanism in various diseases, and practical application of developed PB. We comprehensively examined pertinent academic publications published from January 2019–December 2024 (content 4&5). We exclusively included manuscripts that were authored in English and published in esteemed peer-reviewed journals.

CRediT authorship contribution statement

Hee-Young Kwon: Conceptualization, Investigation, Methodology, Writing – original draft. **Yuna Jung:** Conceptualization, Methodology, Writing – original draft. **Hojeong Jeon:** Supervision, Validation. **Hyung-Seop Han:** Conceptualization, Investigation, Supervision, Writing – original draft.

Declaration of competing interest

Hyung-Seop Han is an editorial board member for Bioactive Materials and was not involved in the editorial review or decision to publish this article. The authors declare no conflicts of interest or personal relationships that could influence this work.

Acknowledgement

This work was supported by the Technology development Program (RS-2024-00506838) funded by the Ministry of SMEs and Startups (MSS, Korea), a National Research Foundation of Korea (NRF) grant funded by the Korean government (MSIT) [grant number RS-2024-00407234] and the KU-KIST Graduate School of Converging Science and Technology Program. Figures were created using BioRender.com.

References

[1] L. Coleby, A history of Prussian blue, Ann. Sci. 4 (2) (1939) 206–211.
[2] M.J.P. Muñoz, E.C. Martínez, Prussian Blue Based Batteries, Springer, 2018.
[3] M. Pyrasch, B. Tieke, Electro-and photoresponsive films of Prussian blue prepared upon multiple sequential adsorption, Langmuir 17 (24) (2001) 7706–7709.
[4] A.A. Karyakin, Prussian blue and its analogues: electrochemistry and analytical applications, Electroanalysis: An International Journal Devoted to Fundamental and Practical Aspects of Electroanalysis 13 (10) (2001) 813–819.
[5] H. Yi, et al., Structure and properties of Prussian blue analogues in energy storage and conversion applications, Adv. Funct. Mater. 31 (6) (2021) 2006970.
[6] W.J. Li, et al., Chemical properties, structural properties, and energy storage applications of Prussian blue analogues, Small 15 (32) (2019) 1900470.
[7] E.S. Goda, et al., Prussian blue and its analogues as advanced supercapacitor electrodes, J. Energy Chem. 50 (2020) 206–229.
[8] Z. Qin, Y. Li, N. Gu, Progress in applications of Prussian blue nanoparticles in biomedicine, Adv. Healthcare Mater. 7 (20) (2018) 1800347.
[9] K. Lu, et al., Progress in the preparation of Prussian blue-based nanomaterials for biomedical applications, J. Mater. Chem. B 11 (24) (2023) 5272–5300.
[10] X. Wang, L. Cheng, Multifunctional Prussian blue-based nanomaterials: preparation, modification, and theranostic applications, Coord. Chem. Rev. 419 (2020) 213393.
[11] Q. Liu, et al., A review on metal-and metal oxide-based nanozymes: properties, mechanisms, and applications, Nano-Micro Lett. 13 (2021) 1–53.
[12] H. Wang, K. Wan, X. Shi, Recent advances in nanozyme research, Adv. Mater. 31 (45) (2019) 1805368.
[13] Y. Lv, et al., Carbon dot nanozymes: how to be close to natural enzymes, Chem.–Eur. J. 25 (4) (2019) 954–960.
[14] J. Yang, Y.W. Yang, Metal–organic frameworks for biomedical applications, Small 16 (10) (2020) 1906846.
[15] Z. Wang, et al., Biosafety and biocompatibility assessment of Prussian blue nanoparticles in vitro and in vivo, Nanomedicine 15 (27) (2020) 2655–2670.
[16] P. Insert, Radiogardase®-Cs Insoluble Prussian Blue (Ferric Hexacyanoferrate, Fe4 [Fe (CN) 6] 3), 2007.
[17] K. Brieger, et al., Reactive oxygen species: from health to disease, Swiss Med. Wkly. 142 (3334) (2012) w13659-w13659.
[18] A.A. Alfadda, R.M. Sallam, Reactive oxygen species in health and disease, BioMed Res. Int. 2012 (1) (2012) 936486.
[19] W. Zhang, et al., Prussian blue nanoparticles as multienzyme mimetics and reactive oxygen species scavengers, J. Am. Chem. Soc. 138 (18) (2016) 5860–5865.
[20] T.S. Leyane, S.W. Jere, N.N. Houreld, Oxidative stress in ageing and chronic degenerative pathologies: molecular mechanisms involved in counteracting oxidative stress and chronic inflammation, Int. J. Mol. Sci. 23 (13) (2022) 7273.
[21] M. Schieber, Navdeep S. Chandel, ROS function in redox signaling and oxidative stress, Curr. Biol. 24 (10) (2014) R453–R462.
[22] S. Di Meo, et al., Role of ROS and RNS sources in physiological and pathological conditions, Oxid. Med. Cell. Longev. 2016 (1) (2016) 1245049.
[23] P. Sharma, et al., Reactive oxygen species, oxidative damage, and antioxidative defense mechanism in plants under stressful conditions, J. Botany 2012 (1) (2012) 217037.
[24] L. He, et al., Antioxidants maintain cellular redox homeostasis by elimination of reactive oxygen species, Cell. Physiol. Biochem. 44 (2) (2017) 532–553.
[25] K. Brieger, et al., Reactive oxygen species: from health to disease, Swiss Med. Wkly. 142 (3334) (2012) w13659.
[26] A. Bhattacharyya, et al., Oxidative stress: an essential factor in the pathogenesis of gastrointestinal mucosal diseases, Physiol. Rev. 94 (2) (2014) 329–354.
[27] L. Zhang, et al., Biochemical basis and metabolic interplay of redox regulation, Redox Biol. 26 (2019) 101284.
[28] C.M.C. Andrés, et al., Superoxide anion chemistry—its role at the core of the innate immunity, Int. J. Mol. Sci. 24 (3) (2023) 1841.

[29] A.J.P.O. de Almeida, et al., ROS: basic concepts, sources, cellular signaling, and its implications in aging pathways, Oxid. Med. Cell. Longev. 2022 (1) (2022) 1225578.
[30] G.-Y. Liou, P. Storz, Reactive oxygen species in cancer, Free Radic. Res. 44 (5) (2010) 479–496.
[31] K. Jomova, et al., Reactive oxygen species, toxicity, oxidative stress, and antioxidants: chronic diseases and aging, Arch. Toxicol. 97 (10) (2023) 2499–2574.
[32] U.C. Dash, et al., Oxidative stress and inflammation in the pathogenesis of neurological disorders: mechanisms and implications, Acta Pharm. Sin. B (2024).
[33] H.J. Forman, H. Zhang, Targeting oxidative stress in disease: promise and limitations of antioxidant therapy, Nat. Rev. Drug Discov. 20 (9) (2021) 689–709.
[34] K. Jomova, et al., Several lines of antioxidant defense against oxidative stress: antioxidant enzymes, nanomaterials with multiple enzyme-mimicking activities, and low-molecular-weight antioxidants, Arch. Toxicol. 98 (5) (2024) 1323–1367.
[35] P. Chaudhary, et al., Oxidative stress, free radicals and antioxidants: potential crosstalk in the pathophysiology of human diseases, Front. Chem. 11 (2023).
[36] G.J. Burton, E. Jauniaux, Oxidative stress, Best Pract. Res. Clin. Obstet. Gynaecol. 25 (3) (2011) 287–299.
[37] N.K. Bhol, et al., The interplay between cytokines, inflammation, and antioxidants: mechanistic insights and therapeutic potentials of various antioxidants and anti-cytokine compounds, Biomed. Pharmacother. 178 (2024) 117177.
[38] Y. Hong, et al., Reactive oxygen species signaling and oxidative stress: transcriptional regulation and evolution, Antioxidants 13 (3) (2024) 312.
[39] B. Poljsak, D. Šuput, I. Milisav, Achieving the balance between ROS and antioxidants: when to use the synthetic antioxidants, Oxid. Med. Cell. Longev. 2013 (1) (2013) 956792.
[40] M. Sharifi-Rad, et al., Lifestyle, oxidative stress, and antioxidants: back and forth in the pathophysiology of chronic diseases, Front. Physiol. 11 (2020).
[41] A.B. Jena, et al., Cellular Red-Ox system in health and disease: the latest update, Biomed. Pharmacother. 162 (2023) 114606.
[42] S. Maity, et al., Oxidative homeostasis regulates the response to reductive endoplasmic Reticulum stress through translation control, Cell Rep. 16 (3) (2016) 851–865.
[43] H. Sies, Chapter 1 - oxidative eustress and oxidative distress: introductory remarks, in: H. Sies (Ed.), Oxidative Stress, Academic Press, 2020, pp. 3–12.
[44] H. Sies, Oxidative eustress: on constant alert for redox homeostasis, Redox Biol. 41 (2021) 101867.
[45] H. Sies, Oxidative eustress: the physiological role of oxidants, Sci. China Life Sci. 66 (8) (2023) 1947–1948.
[46] A.M. Pisoschi, et al., Oxidative stress mitigation by antioxidants - an overview on their chemistry and influences on health status, Eur. J. Med. Chem. 209 (2021) 112891.
[47] E. Birben, et al., Oxidative stress and antioxidant defense, World Allergy Organiz. J. 5 (1) (2012) 9–19.
[48] M. Pyrasch, B. Tieke, Electro- and photoresponsive films of prussian blue prepared upon multiple sequential adsorption, Langmuir 17 (24) (2001) 7706–7709.
[49] M. Cammarata, et al., Charge transfer driven by ultrafast spin transition in a CoFe Prussian blue analogue, Nat. Chem. 13 (1) (2021) 10–14.
[50] E.S. Koumousi, et al., Metal-to-Metal electron transfer in Co/Fe prussian blue molecular analogues: the ultimate miniaturization, J. Am. Chem. Soc. 136 (44) (2014) 15461–15464.
[51] I.A. Salem, M. El-Maazawi, A.B. Zaki, Kinetics and mechanisms of decomposition reaction of hydrogen peroxide in presence of metal complexes, Int. J. Chem. Kinet. 32 (11) (2000) 643–666.
[52] L. Gao, et al., Intrinsic peroxidase-like activity of ferromagnetic nanoparticles, Nat. Nanotechnol. 2 (9) (2007) 577–583.
[53] X.-Q. Zhang, et al., Prussian blue modified iron oxide magnetic nanoparticles and their high peroxidase-like activity, J. Mater. Chem. 20 (24) (2010) 5110–5116.
[54] K. Feng, et al., Elucidating the catalytic mechanism of Prussian blue nanozymes with self-increasing catalytic activity, Nat. Commun. 15 (1) (2024) 5908.
[55] M.B. Zakaria, T. Chikyow, Recent advances in Prussian blue and Prussian blue analogues: synthesis and thermal treatments, Coord. Chem. Rev. 352 (2017) 328–345.
[56] D. Li, et al., Synthesis of prussian blue nanoparticles and their antibacterial, antiinflammation and antitumor applications, Pharmaceuticals 15 (7) (2022) 769.
[57] S. Kjeldgaard, et al., Strategies for synthesis of Prussian blue analogues, R. Soc. Open Sci. 8 (1) (2021) 201779.
[58] M. Shukla, et al., A review on tunable multi-functional Prussian blue nanoparticles; their promising biological applications & future directions, Coord. Chem. Rev. 496 (2023) 215414.
[59] S. Fan, et al., The design and synthesis of Prussian blue analogs as a sustainable cathode for sodium-ion batteries, SusMat 3 (6) (2023) 749–780.
[60] Y. Yue, et al., Mesoporous prussian blue analogues: template-free synthesis and sodium-ion battery applications, Angew. Chem. Int. Ed. 53 (12) (2014) 3134–3137.
[61] G. Du, H. Pang, Recent advancements in Prussian blue analogues: preparation and application in batteries, Energy Storage Mater. 36 (2021) 387–408.
[62] J. Estelrich, M.A. Busquets, Prussian blue: a nanozyme with versatile catalytic properties, Int. J. Mol. Sci. 22 (11) (2021) 5993.
[63] V. Hornok, I. Dékány, Synthesis and stabilization of Prussian blue nanoparticles and application for sensors, J. Colloid Interface Sci. 309 (1) (2007) 176–182.
[64] Q. Wang, et al., Prussian-blue materials: revealing new opportunities for rechargeable batteries, InfoMat 4 (6) (2022) e12311.
[65] L.-M. Cao, et al., Prussian blue analogues and their derived nanomaterials for electrocatalytic water splitting, Coord. Chem. Rev. 407 (2020) 213156.
[66] C. Li, et al., Fundamental understanding of Prussian blue and its analogues for superior capacitive deionization: a perspective from nanoarchitectonics, Coord. Chem. Rev. 520 (2024) 216100.
[67] B. Bornamehr, et al., Prussian blue and its analogues as functional template materials: control of derived structure compositions and morphologies, J. Mater. Chem. A 11 (20) (2023) 10473–10492.
[68] P. Khramtsov, et al., Synthesis of Prussian Blue nanoparticles in water/alcohol mixtures, Colloids Surf. A Physicochem. Eng. Asp. 686 (2024) 133446.
[69] M.J. Mitchell, et al., Engineering precision nanoparticles for drug delivery, Nat. Rev. Drug Discov. 20 (2) (2021) 101–124.
[70] H. Ming, et al., Size- and shape-controlled synthesis of Prussian Blue nanoparticles by a polyvinylpyrrolidone-assisted crystallization process, CrystEngComm 14 (10) (2012) 3387–3396.
[71] X. Shen, et al., Morphology syntheses and properties of well-defined Prussian Blue nanocrystals by a facile solution approach, J. Colloid Interface Sci. 329 (1) (2009) 188–195.
[72] T. Uemura, M. Ohba, S. Kitagawa, Size and surface effects of prussian blue nanoparticles protected by organic polymers, Inorg. Chem. 43 (23) (2004) 7339–7345.
[73] Y. Wang, et al., Advancements of Prussian blue-based nanoplatforms in biomedical fields: progress and perspectives, J. Contr. Release 351 (2022) 752–778.
[74] M.A. Busquets, J. Estelrich, Prussian blue nanoparticles: synthesis, surface modification, and biomedical applications, Drug Discov. Today 25 (8) (2020) 1431–1443.
[75] X. Chen, et al., Engineering ROS-scavenging Prussian blue nanozymes for efficient atherosclerosis nanotherapy, J. Mater. Chem. B 11 (9) (2023) 1881–1890.
[76] R. Hou, et al., Prussian blue nanozyme promotes the survival rate of skin flaps by maintaining a normal microenvironment, ACS Nano 16 (6) (2022) 9559–9571.
[77] T. Zhou, et al., Prussian blue nanoparticles stabilize SOD1 from ubiquitination-proteasome degradation to rescue intervertebral disc degeneration, Adv. Sci. 9 (10) (2022) 2105466.
[78] H. Bai, et al., Prussian blue nanozymes prevent anthracycline-induced liver injury by attenuating oxidative stress and regulating inflammation, ACS Appl. Mater. Interfaces 13 (36) (2021) 42382–42395.
[79] J. Liu, et al., Prussian blue nanozyme treatment of ischemic brain injury via reducing oxidative stress inhibits inflammation, suppresses apoptosis, and promotes neurological recovery, ACS Chem. Neurosci. 14 (8) (2023) 1535–1546.
[80] X. Ma, et al., Prussian blue nanozyme as a pyroptosis inhibitor alleviates neurodegeneration, Adv. Mater. 34 (15) (2022) 2106723.
[81] Z. Qin, et al., Ultrasmall prussian blue nanozyme attenuates osteoarthritis by scavenging reactive oxygen species and regulating macrophage phenotype, Nano Lett. 24 (37) (2024) 11697–11705.
[82] L. Feng, et al., Neutrophil-like cell-membrane-coated nanozyme therapy for ischemic brain damage and long-term neurological functional recovery, ACS Nano 15 (2) (2021) 2263–2280.
[83] Y. Zhao, et al., Polydopamine-cloaked nanoarchitectonics of prussian blue nanoparticles promote functional recovery in neonatal and adult ischemic stroke models, Biomater. Res. 28 (2024) 79.
[84] H. Zhou, et al., Artemisinin and Procyanidins loaded multifunctional nanocomplexes alleviate atherosclerosis via simultaneously modulating lipid influx and cholesterol efflux, J. Contr. Release 341 (2022) 828–843.
[85] Y. Liu, et al., Reprogramming monocytes into M2 macrophages as living drug depots to enhance treatment of myocardial ischemia-reperfusion injury, J. Contr. Release 374 (2024) 639–652.
[86] Y. Zhang, et al., Reactive oxygen species scavenging and inflammation mitigation enabled by biomimetic prussian blue analogues boycott atherosclerosis, J. Nanobiotechnol. 19 (1) (2021) 161.
[87] Q. Wang, et al., Sodium salt assisted room-temperature synthesis of Prussian blue analogues as high-performance cathodes for sodium-ion batteries, Appl. Surf. Sci. 669 (2024) 160499.
[88] J. Kowalczyk, et al., Dual effect of prussian blue nanoparticles on Aβ40 aggregation: β-Sheet fibril reduction and copper dyshomeostasis regulation, Biomacromolecules 22 (2) (2021) 430–440.
[89] J. Zhao, et al., Nanozyme-mediated catalytic nanotherapy for inflammatory bowel disease, Theranostics 9 (10) (2019) 2843.
[90] L. Li, et al., Biofilm-camouflaged Prussian blue synergistic mitochondrial mass enhancement for Alzheimer's disease based on Cu2+ chelation and photothermal therapy, J. Contr. Release 375 (2024) 269–284.
[91] A. Tong, et al., Prussian blue nano-enzyme-assisted photodynamic therapy effectively eradicates MRSA infection in diabetic mouse skin wounds, Biomater. Sci. 11 (18) (2023) 6342–6356.
[92] W. Zhang, et al., Platelet membrane-functionalized hollow mesoporous Prussian blue nanomedicine for comprehensive thrombolytic management by targeted enhanced fibrinolysis and ROS scavenging, Chem. Eng. J. 474 (2023) 145515.
[93] W. Zhang, et al., Antithrombotic therapy by regulating the ROS-mediated thrombosis microenvironment and specific nonpharmaceutical thrombolysis using prussian blue nanodroplets, Small 18 (15) (2022) 2106252.
[94] K. Shen, et al., High rapamycin-loaded hollow mesoporous Prussian blue nanozyme targets lesion area of spinal cord injury to recover locomotor function, Biomaterials 303 (2023) 122358.

[95] D.-Y. Zhang, et al., Prussian blue-based theranostics for ameliorating acute kidney injury, J. Nanobiotechnol. 19 (2021) 1–14.
[96] X.-J. Zheng, et al., Growth of prussian blue microcubes under a hydrothermal condition: possible nonclassical crystallization by a mesoscale self-assembly, J. Phys. Chem. C 111 (12) (2007) 4499–4502.
[97] D.A. Peixoto, et al., Hydrothermal synthesis as a versatile tool for the preparation of metal hexacyanoferrates: a review, J. Mater. Sci. 58 (7) (2023) 2993–3024.
[98] J. Yang, D.H. Li, L.L. Ji, A low-temperature hydrothermal synthesis of prussian blue nanocrystal and its application in H2O2 detection, J. Chem. 2022 (1) (2022) 7593873.
[99] S. Ying, et al., Synthesis and applications of prussian blue and its analogues as electrochemical sensors, ChemPlusChem 86 (12) (2021) 1608–1622.
[100] M. Ruiz-Bermejo, et al., Thermal wet decomposition of prussian blue: implications for prebiotic chemistry, Chem. Biodivers. 6 (9) (2009) 1309–1322.
[101] L. Wang, et al., Rhombohedral prussian white as cathode for rechargeable sodium-ion batteries, J. Am. Chem. Soc. 137 (7) (2015) 2548–2554.
[102] Y. You, et al., Subzero-temperature cathode for a sodium-ion battery, Adv. Mater. 28 (33) (2016) 7243–7248.
[103] C. Ye, et al., Prussian blue nanozyme normalizes microenvironment to delay osteoporosis, Adv. Healthcare Mater. 11 (19) (2022) 2200787.
[104] X. Song, et al., Peptide-functionalized prussian blue nanomaterial for antioxidant stress and NIR photothermal therapy against alzheimer's disease, Small 19 (41) (2023) 2206959.
[105] J. Xie, et al., Liposome-loaded Prussian blue nanoparticles accelerate wound healing by promoting anti-inflammatory effects, New J. Chem. 48 (21) (2024) 9542–9548.
[106] D.-X. Tang, et al., Artificial nonenzymatic antioxidant Prussian blue/KGM-BSA nanocomposite hydrogel dressing as ROS scavenging for diabetic wound healing, Int. J. Biol. Macromol. (2024) 131106.
[107] B. Zhang, et al., Biomimetic Prussian blue nanozymes with enhanced bone marrow-targeting for treatment of radiation-induced hematopoietic injury, Biomaterials 293 (2023) 121980.
[108] Y.-R. Ji, et al., Insights on rational design and regulation strategies of Prussian blue analogues and their derivatives towards high-performance electrocatalysts, Chem. Eng. J. 471 (2023) 144743.
[109] S. Vaucher, M. Li, S. Mann, Synthesis of prussian blue nanoparticles and nanocrystal superlattices in reverse microemulsions, Angew. Chem. Int. Ed. 39 (10) (2000) 1793–1796.
[110] Z. Xu, et al., Thermosensitive hydrogel incorporating Prussian blue nanoparticles promotes diabetic wound healing via ROS scavenging and mitochondrial function restoration, ACS Appl. Mater. Interfaces 14 (12) (2022) 14059–14071.
[111] Z. Wang, et al., Ion-exchange synthesis of high-energy-density prussian blue analogues for sodium ion battery cathodes with fast kinetics and long durability, J. Power Sources 436 (2019) 226868.
[112] M. Hirai, et al., Characteristics of AOT microemulsion structure depending on apolar solvents, J. Phys. Chem. B 103 (44) (1999) 9658–9662.
[113] J. Texter, et al., Polymerizable bis(2-ethylhexyl)sulfosuccinate: application in microemulsion polymerization, Langmuir 20 (26) (2004) 11288–11292.
[114] E.B. Abuin, M.A. Rubio, E.A. Lissi, Solubility of water in water-in-oil microemulsions stabilized by cetyltrimethylammonium: effects of the surfactant counterion, the nature and composition of the oil, and the salinity of the droplets, J. Colloid Interface Sci. 158 (1) (1993) 129–132.
[115] Y. Huang, et al., Prussian blue scavenger ameliorates hepatic ischemia-reperfusion injury by inhibiting inflammation and reducing oxidative stress, Front. Immunol. 13 (2022) 891351.
[116] D. Zhu, et al., Zero-valence selenium-enriched Prussian blue nanozymes reconstruct intestinal barrier against inflammatory bowel disease via inhibiting Ferroptosis and T cells differentiation, Adv. Healthcare Mater. 12 (12) (2023) 2203160.
[117] C. Procaccini, et al., Role of metabolism in neurodegenerative disorders, Metabolism 65 (9) (2016) 1376–1390.
[118] M.T. Islam, Oxidative stress and mitochondrial dysfunction-linked neurodegenerative disorders, Neurol. Res. 39 (1) (2017) 73–82.
[119] S. Bhatt, L. Puli, C.R. Patil, Role of reactive oxygen species in the progression of Alzheimer's disease, Drug Discov. Today 26 (3) (2021) 794–803.
[120] M. Weng, et al., The sources of reactive oxygen species and its possible role in the pathogenesis of Parkinson's disease, Parkinson's Dis. 2018 (1) (2018) 9163040.
[121] E. Lee, et al., MPTP-driven NLRP3 inflammasome activation in microglia plays a central role in dopaminergic neurodegeneration, Cell Death Differ. 26 (2) (2019) 213–228.
[122] P.A. Lapchak, Stroke therapy development successes: research guidelines and embolic stroke models for monotherapy and adjuvant therapy development, in: P. A. Lapchak, G.-Y. Yang (Eds.), Translational Research in Stroke, Springer Singapore, Singapore, 2017, pp. 3–27.
[123] D.S.A. Simpson, P.L. Oliver, ROS generation in microglia: understanding oxidative stress and inflammation in neurodegenerative disease, Antioxidants 9 (8) (2020) 743.
[124] J. Palasubramaniam, X. Wang, K. Peter, Myocardial infarction—from atherosclerosis to thrombosis, Arterioscler. Thromb. Vasc. Biol. 39 (8) (2019) e176–e185.
[125] K. Sugamura, J.F. Keaney, Reactive oxygen species in cardiovascular disease, Free Radic. Biol. Med. 51 (5) (2011) 978–992.
[126] M. Algoet, et al., Myocardial ischemia-reperfusion injury and the influence of inflammation, Trends Cardiovasc. Med. 33 (6) (2023) 357–366.
[127] N. Mackman, Triggers, targets and treatments for thrombosis, Nature 451 (7181) (2008) 914–918.
[128] A.J. Kattoor, et al., Oxidative stress in atherosclerosis, Curr. Atheroscler Rep. 19 (11) (2017) 42.
[129] W. Zhang, et al., Platelet membrane-functionalized hollow mesoporous Prussian blue nanomedicine for comprehensive thrombolytic management by targeted enhanced fibrinolysis and ROS scavenging, Chem. Eng. J. 474 (2023) 145515.
[130] T. Kalogeris, et al., Chapter six - cell biology of ischemia/reperfusion injury, in: K. W. Jeon (Ed.), International Review of Cell and Molecular Biology, Academic Press, 2012, pp. 229–317.
[131] E.R. Sherwood, T. Toliver-Kinsky, Mechanisms of the inflammatory response, Best Pract. Res. Clin. Anaesthesiol. 18 (3) (2004) 385–405.
[132] S.J. Forrester, et al., Reactive oxygen species in metabolic and inflammatory signaling, Circ. Res. 122 (6) (2018) 877–902.
[133] G.I. Broughton, J.E. Janis, C.E. Attinger, The basic science of wound healing, Plast. Reconstr. Surg. 117 (7S) (2006) 12S–34S.
[134] L. Deng, et al., The role of oxidative stress and antioxidants in diabetic wound healing, Oxid. Med. Cell. Longev. 2021 (1) (2021) 8852759.
[135] K.P. Pavlick, et al., Role of reactive metabolites of oxygen and nitrogen in inflammatory bowel disease, Free Radic. Biol. Med. 33 (3) (2002) 311–322.
[136] E. Jimi, et al., The current and future therapies of bone regeneration to repair bone defects, Int. J. Dentistr. 2012 (1) (2012) 148261.
[137] A.E. Bădilă, et al., Bone regeneration and oxidative stress: an updated overview, Antioxidants 11 (2) (2022) 318.
[138] C. Feng, et al., ROS: crucial intermediators in the pathogenesis of intervertebral disc degeneration, Oxid. Med. Cell. Longev. 2017 (1) (2017) 5601593.
[139] J.M. Dennis, P.K. Witting, Protective role for antioxidants in acute kidney disease, Nutrients 9 (7) (2017) 718.
[140] E.J. Bradbury, E.R. Burnside, Moving beyond the glial scar for spinal cord repair, Nat. Commun. 10 (1) (2019) 3879.
[141] A. Anjum, et al., Spinal cord injury: pathophysiology, multimolecular interactions, and underlying recovery mechanisms, Int. J. Mol. Sci. 21 (20) (2020) 7533.
[142] Y. Li, et al., Mitochondrial dysfunction and oxidative stress in bone marrow stromal cells induced by daunorubicin leads to DNA damage in hematopoietic cells, Free Radic. Biol. Med. 146 (2020) 211–221.
[143] N. Desai, Challenges in development of nanoparticle-based therapeutics, AAPS J. 14 (2) (2012) 282–295.
[144] W. Najahi-Missaoui, R.D. Arnold, B.S. Cummings, Safe nanoparticles: are we there yet? Int. J. Mol. Sci. 22 (1) (2021) 385.
[145] J.K. Patra, et al., Nano based drug delivery systems: recent developments and future prospects, J. Nanobiotechnol. 16 (1) (2018) 71.
[146] I. Khan, K. Saeed, I. Khan, Nanoparticles: properties, applications and toxicities, Arab. J. Chem. 12 (7) (2019) 908–931.
[147] G. De Crozals, et al., Nanoparticles with multiple properties for biomedical applications: a strategic guide, Nano Today 11 (4) (2016) 435–463.
[148] T.R. Kyriakides, et al., Biocompatibility of nanomaterials and their immunological properties, Biomed. Mater. 16 (4) (2021) 042005.
[149] S.P. Mankoff, et al., Lost in translation: obstacles to translational medicine, J. Transl. Med. 2 (1) (2004) 14.
[150] L.-P. Wu, D. Wang, Z. Li, Grand challenges in nanomedicine, Mater. Sci. Eng. C 106 (2020) 110302.
[151] A. Mohammad, et al., A long-term stability study of Prussian blue: a quality assessment of water content and cesium binding, J. Pharmaceut. Biomed. Anal. 103 (2015) 85–90.
[152] A. Mohammad, et al., Long-term stability study of Prussian blue – a quality assessment of water content and thallium binding, Int. J. Pharm. 477 (1) (2014) 122–127.
[153] M. Shokouhimehr, et al., Biocompatible Prussian blue nanoparticles: preparation, stability, cytotoxicity, and potential use as an MRI contrast agent, Inorg. Chem. Commun. 13 (1) (2010) 58–61.
[154] M. Shokouhimehr, et al., Dual purpose Prussian blue nanoparticles for cellular imaging and drug delivery: a new generation of T1-weighted MRI contrast and small molecule delivery agents, J. Mater. Chem. 20 (25) (2010) 5251–5259.
[155] G. Fu, et al., Prussian blue nanoparticles operate as a new generation of photothermal ablation agents for cancer therapy, Chem. Commun. 48 (94) (2012) 11567–11569.
[156] Y. Chen, et al., Toxicological evaluation of Prussian blue nanoparticles after short exposure of mice, Hum. Exp. Toxicol. 35 (10) (2015) 1123–1132.